Impedance Measurement platform for Impedimetric biosensor

By

Gerard Bamuturaki Kato

Submitted to the Department of Electrical Engineering and Computer Science

On May 21, 2015, in partial fulfillment of the

requirement for the degree of

Master of Engineering in Electrical Engineering and Computer Science

at the

MASSACHUSETTS INSTITUTE OF TECHNOLOGY

June 2015

Author ……

Department of Electrical Engineering and Computer Science
May 21, 2014

Certified by ……

Professor Joel Voldman
Department of Electrical Engineering and Computer Science
Thesis Supervisor

Certified by ……

Brian Brandt
Distinguished Member of Technical Staff, Maxim Integrated Products
Thesis Supervisor

Accepted by ……

Prof. Albert R. Meyer
Chairman, Masters of Engineering Thesis committee

Impedance Measurement platform for Impedimetric biosensor

By

Gerard Bamuturaki Kato

Submitted to the Department of Electrical Engineering and Computer Science

On May 21, 2015, in partial fulfillment of the

requirement for the degree of

Master of Engineering in Electrical Engineering and Computer Science

Abstract

Measuring proteins in blood is particularly common such as in PSA, to determine prostate function and in many other bio-applications. Today this process is inconveniencing in that it requires a lot of blood from the patients for tests to be made. Furthermore it is time consuming and expensive since samples are transferred to a central lab where tests are carried out on optical assays.

Using electrical read out methods several measurements can be multiplexed and a differential measurements made. With a differential measurement the precision of the system is improved by cancelling out common mode bio-chemical noise. The multiplexed measurement enables measurement of several analytes. Using the embedded system MAX32600, an electrical impedance meter was designed that measures three impedances simultaneously with accuracy range of up-to 1% and precision of 0.2% of the actual impedance measured from an Impedance analyzer.

Thesis Supervisor: Brian Brandt
Title: Distinguished Member of Technical Staff, Maxim Integrated Products

Thesis Supervisor: Joel Voldman
Title: Professor, Department of Electrical Engineering and Computer Science

Acknowledgements

I would like to thank Maxim Integrated for sponsoring my Masters of Engineering project. I am grateful for both the financial contribution from Maxim in form of tuition fees but also the offered stipends helped me meet my daily needs during this period. Working next to the top engineers at Maxim made the learning process even more fun. I am especially grateful to my thesis supervisor at Maxim Integrated Brian Brandt. Brian was not only extremely helpful in defining my thesis work but also helped me at points I reached deadlocks. The weekly meetings helped define the project better and keep track of my project. I am grateful that you offered your time to come to the lab and help me debug my circuits. I also appreciate the advice about the next steps after graduation.

I am also thankful to my undergraduate VI-A advisor from Maxim Integrated Patrick Coady. Thanks Pat for the help and time offered during my first internship. I had a very interesting and challenging project for the first internship. This raised my curiosity and love for analog circuit design. At Maxim I am also grateful for the help from other engineers John Di Cristina, Kevin Witt, Diana Carrigan for the help with code on the MAX32600 board.

Next I am very thankful to MIT for the VI-A program and the process to link students with companies to gain industry experience while completing a Master's degree. I would also like to thank Kathy Sullivan for the help when I had any questions about how the VI-A program works.

At MIT also I would like to thank my thesis advisor Joel Voldman. I am grateful for the help in tracking my project progress and advice while writing up the thesis. Thank you for letting me join you group and mentoring me in the process. I thank Dan Wu for the help with the running experiments in lab, designing the GUI and advice.

I can't forget to thank my family for the help throughout my life. I am thankful to my parents for educating me and sacrificing a lot for me to attain the best in life. I also thank my twin brother George Kakuru for all his support. Thank you so much for the sacrifices and all the life lessons you have offered.

Last but not least I thank God for the blessings and love offered. I am thankful for all the blessings offered throughout my life.

Contents

Impedance Measurement platform for Impedimetric biosensor 1
Impedance Measurement platform for Impedimetric biosensor 2
Abstract 2
Chapter 1: Biosensors and Electrical Read-out 8
1.1 Objective and Approach 8
1.2 Definition of a biosensor 8
1.3 Characteristics of good biosensors 10
1.3.1 Selectivity 10
1.3.2 Non Specific binding 10
1.3.2 Differential Sensor 10
1.3.3 Multiplexing ability 11
1.3.4 Reproducibility and sensitivity 11
1.4 Point of Care Testing 12
1.5 Electrical biosensors 13
1.6 Impedimetric Biosensor 14
1.6.1 Model of an Impedimetric biosensor 14
1.6.2 Electrical Readout 17
1.7 Previous work on Impedimetric Biosensors 20
1.8 Chapter Conclusion and Thesis Organization 21
Chapter 2: Impedance Measurement System 23
2.1 System Description 23
2.1.1 Signal Generation Stage 24
2.1.2 Attenuation Stage 24
2.1.3 Measurement Stage 25
2.2 Measuring Impedances 27
2.2.1 Choice of Z_f 27
2.2.2 Choice of Z_{CAL} 29
2.2.3 Noise Analysis 31
2.2.4 Op amp Bandwidth 34
2.2.5 Switch Resistance 36

2.3 Impedance meter trade-offs 40
2.4 Conclusions 40
Chapter 3: Impedance and biosensor measurement results 41
3.1 Capacitor Measurements 41
3.2 MATLAB GUI 45
3.2.1: Determination of the Capacitance values and biosensor modelling 46
3.3 Capacitor change measurement 47
3.4 Measuring a Biosensor Impedance 48
3.4.1: Pre-measurement sensor test 49
3.4.2: Building the sensor 50
3.4.3: Actual sensor measurement 51
Chapter 4: Conclusion and Future work **53**
4.1 Summary and contributions **53**
4.2 Future works **53**
Appendix **55**
References **64**

List of Figures

Figure 1: Block Diagram of a Biosensor based on [2] 8
Figure 2: A Block diagram showing a differential measurement 10
Figure 3: Representation of Multiplexing in Biosensors [9] 11
Figure 4: General Model of Impedimetric biosensor 14
Figure 5: Circuit Schematic of an Impedimetric Biosensor [10] 15
Figure 6: Magnitude plot for a typical biosensor 16
Figure 7: Phase plot for a typical biosensor 16
Figure 8: Schematic of the bridge method based on [13] 17
Figure 9: Circuit Schematic of the Resonant Method [13] 18
Figure 10: Circuit Schematic of the I-V Method [13] 18
Figure 11: Circuit Schematic of the Auto-balancing bridge Method [13] 19
Figure 12: Circuit Schematic of the Entire Impedance Measurement setup 23
Figure 13: Plots Showing Precision Variation with Calibration Capacitance 30
Figure 14: Circuit Schematic to determine Noise 32
Figure 15: Output Noise variation with frequency for the setup 32
Figure 16: Circuit Schematic for op amp Bandwidth effects 34
Figure 17: Plots showing the effect of switch resistance on Magnitude and Phase measurements 38
Figure 18: Plot for the Magnitude difference between the uncalibrated and calibrated MAX32600 setup 39
Figure 19: Plot for the phase difference between the uncalibrated and the calibrated MAX32600 setup 39
Figure 20: Picture showing the setup of the MAX32600 to measure 3 Capacitors 41
Figure 21: Magnitude and Phase plots of the Impedance Analyzer and the MAX32600 System for 4.7nF Capacitor 42
Figure 22: Measured capacitance over time for a 4.7nF Capacitor 43
Figure 23: Measured capacitance over time for a 10nF Capacitor 44
Figure 24: Measured capacitance over time for a 32nF Capacitor 44
Figure 25: MATLAB GUI Layout 45
Figure 26: Capacitor change measurement for a 4.91nF Capacitor 47
Figure 27: Capacitor change measurement for a 10.397nF Capacitor 48
Figure 28: Plot showing steps in the pre-measurement sensor checkout step 49
Figure 29: Plot showing steps in building the sensor step 50
Figure 30: Plot showing steps in actual sensor measurement step 51
Figure 31: Capacitor change against antibody concentration 52

List of Figures

Table 1: Comparison of possible Electric biosensors 13
Table 2: Table for the Gain and Phase errors for op amps with different GBP 36
Table 3: Measurement Precision of the MAX32600 for 3 Capacitors 45

Chapter 1: Biosensors and Electrical Read-out

1.1 Objective and Approach

Protein biosensors are becoming highly useful in several applications such as to test liver function and detecting diseases and body function. For this reason an effective, fast and low cost readout method is required for these biosensors. Currently, many systems are based on optical readout techniques where the readout is carried out in a central lab. These optical measurement systems can be bulky, take a long time (usually several days) to carry out tests (since tests are taken at a central lab) and are also expensive due to the optical nature of the assay. To offset the short comings of optical biosensors readout some systems have moved to electrical readout techniques. But even with electrical readout techniques many of the current systems use impedance analyzers to do the measurements. These impedance analyzers although accurate are bulky and expensive. Therefore for fast, low cost, portable design of a biosensor would require moving away from the impedance analyzer to a more portable electronic measurement setup.

The goal of this thesis is to describe an electrical readout technique that uses the MAX32600 board which is an embedded system for biological applications to measure proteins in blood. The advantage with the board level electrical impedance readout system is that on top of being a portable system it presents the ability to measure the impedance differentially and have multiplexed measurements hence increasing the accuracy of the measurement and being able to take several measurements at the same time that lowers costs.

1.2 Definition of a biosensor

According to the IUPAC definition, a biosensor is a self-contained integrated device capable of providing specific quantitative or semi-quantitative analytical information using a biological recognition element (bio-receptor) that is in direct spatial contact with an electrochemical transduction element [1]. Basically a biosensor utilizes biological components such as enzymes and/or antibodies to indicate the amount of a biomaterial such as an antigen [2].

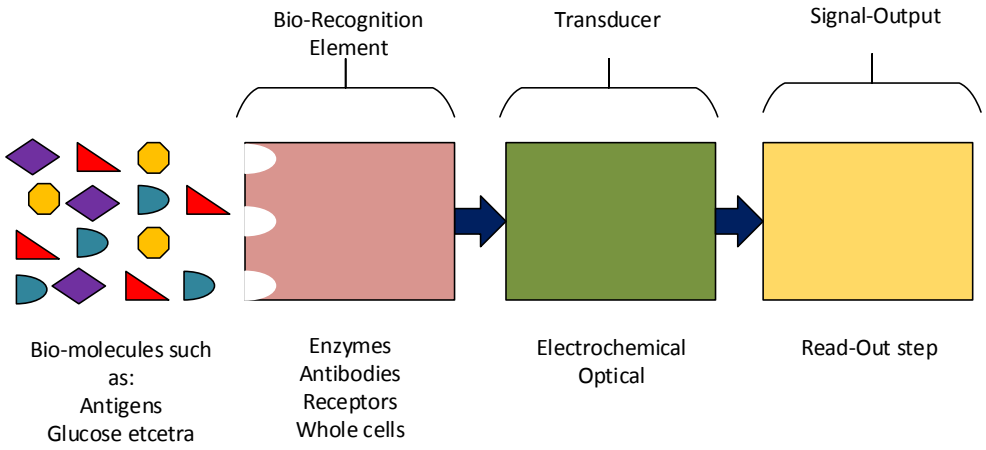

Figure 1: Block Diagram of a Biosensor based on [2]

Shown in the Figure 1 is the block diagram of a general biosensor and all biosensors are based on the block diagram above. The first step in a biosensor is bio-recognition. In this step the bio molecule that needs to be detected gets attached to another bio molecule. This is usually described as a wet process that involves solutions and some form of a chemical reaction. The next step is transduction. This step will involve detecting the previous step using either electrical methods or optical methods. The final step would be the interpretation of the transducer. Interpretation of the transducer could be variable process depending on what is being tested. In some biosensors this step is a binary step where we can decide the presence or absence of the bio-molecule to be detected. A good example for such a biosensor would be in pregnancy tests. In other biosensors such as glucose meters, this step will provide the proportion of the bio-molecule detected available in the solution such as a blood solution.

Biosensors can be classified in several subgroups according to the method used by the transducer. The methods are described further below:

I. Optical biosensors. These biosensors use optical properties to detect the presence of a biomolecule. Under this method lies techniques such as Surface Plasmon Resonance (SPR). In SPR light is shined through a glass slide (that is connected to a thin gold film within to a flow channel) at angles and frequencies near the SPR condition. The optical reflectivity of the gold film changes highly sensitive with the concentration of biomolecule to be detected [3].Fluorescence biosensors, on the other hand, involve excitation of labels at one wavelength and then detecting the photon emission at a different wavelength, where the emission intensity is related to the concentration of labels. Optical detection is still the most sensitive and robust bio-sensing technique. This sensitivity and robustness is attributed to the uniqueness of the fluorescence phenomenon which makes the generated signals specific and less susceptible to biological interference [4]. For this reason optical bio-sensing is currently the most widely used technique although it is expensive and time consuming to do measurement using optical assays. Long *et al.* [5] describe how applications that use optical biosensors for environmental monitoring are still expensive, require trained personnel to operate and motivate the need to develop less expensive biosensors.

II. Mechanical biosensors. This category of biosensors use the mechanical properties of material that change when a bio-molecule is detected. Techniques include the Quartz Crystal Microbalance, which is an acoustic sensor based on a piezoelectric crystal. This method detects mass changes in nanogram range on the sensor that result from the binding of the biomolecule [6]. Another method is the Resonant Cantilever, which consists of cantilevers mechanically excited at their resonant frequency. When the biomolecule is added and it binds to the bio recognition element there is a shift in the resonant frequency of the cantilever causing mechanical deformation of the cantilever [7].

III. Electromagnetic biosensors. These biosensors use the magnetic properties of the bio-materials. Because of the shortcomings of the optical biosensors, magnetically labelled biosensor are one of the suggested solutions to overcome them. Many magnetic biosensors [8] require an external magnetic field, which can increase the size of the biosensor. Wang et al. describe a magnetic biosensor that provides single-bead detection sensitivity without any external magnets [8]. The analytes are detected when the inductance of an integrated resonator changes due to generation of an AC electrical current. This change in inductance of the resonator results in a change in the oscillation frequency, which can be determined electronically [8].

IV. Electrical biosensors. Electrical biosensors rely on the measurement of electrical current and/or voltage to detect binding [1]. Electrical biosensors have shown promise in key characteristics of biosensors such as the ability to multiplex several measurements, the ability to do a differential measurement, reduced cost, and power reduction. The rest of this thesis is going to discuss this approach to biosensor that is becoming an attractive method.

1.3 Characteristics of good biosensors

For a biosensor to detect an analyte with a high accuracy there are some characteristics that it should have. This section presents some of these characteristics:

1.3.1 Selectivity

Selectivity is defined as the ability of a biosensor to react to a particular analyte and not to any other analytes. This is an important characteristic that makes it possible for biosensors to accurately determine the concentration of a specific analyte and no other analytes. Antigen-Antibody interaction has the highest selectivity because it is analyte-specific [9].

1.3.2 Non Specific binding

A characteristic similar to selectivity is ability of the biosensor to ignore non-specific binding. Nonspecific binding is the binding of an analyte that is not the one supposed to be detected resulting in a false positive signal. This kind of binding is usually weak although they affect the readout values. In order to eliminate the effects of nonspecific binding since the binding is weak, a wash step is used to wash away the nonspecific elements that bind to the bio-recognition element. This wash step will leave only the specifically bound elements resulting in the determination of the concentration of the analyte to be determined.

1.3.2 Differential Sensor

In real systems there are several sources of noise. One form of noise can be associated with the biological common mode noise sources such as temperature changes, difference in pH and several other sources. In order to avoid measurements in signals resulting from such common mode biological noises a differential measurement might be required.

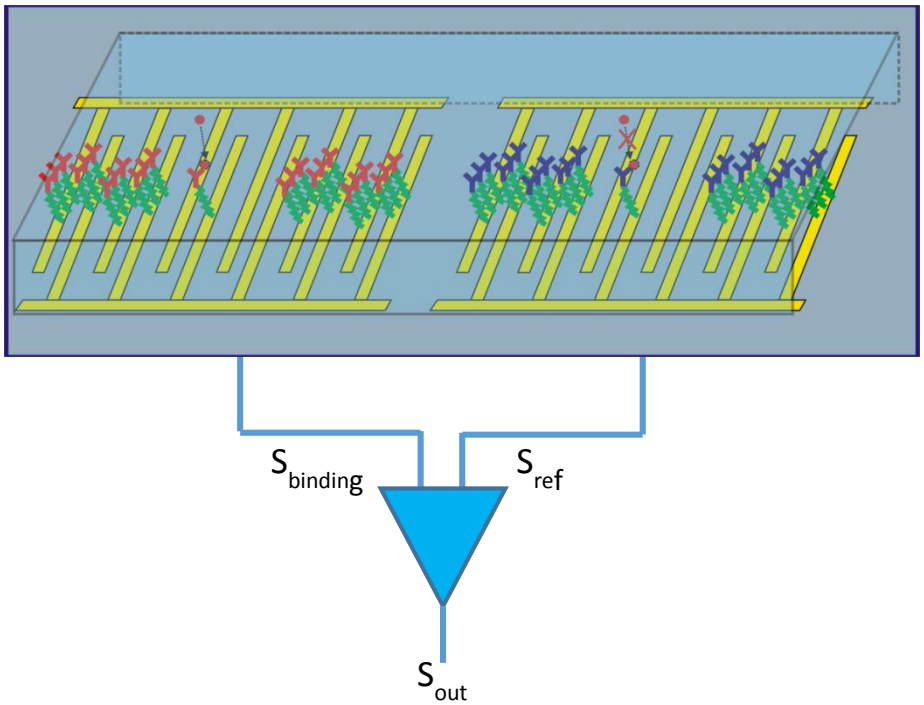

Figure 2: A Block diagram showing a differential measurement

Figure 2 above shows how a differential measurement can be carried out. Two sensors are used. One of the sensors is the binding electrode that consists of the bio-recognition element to which the analyte will bind so it can be determined. The other sensor is the control electrode (or reference electrode), this one does not contain the bio-recognition element and when the analyte is added no binding occurs and therefore the signal change that results in this sensor is a result of the biological common mode signals such as pH changes, temperature changes The active electrode is shown on the left of the figure and the control electrode is on the right. The figure shows when the analyte is added, it only binds on the active electrode. Doing a differential measurement of these two signals will result in determination of the signal that results only from the binding of the analyte.

1.3.3 Multiplexing ability

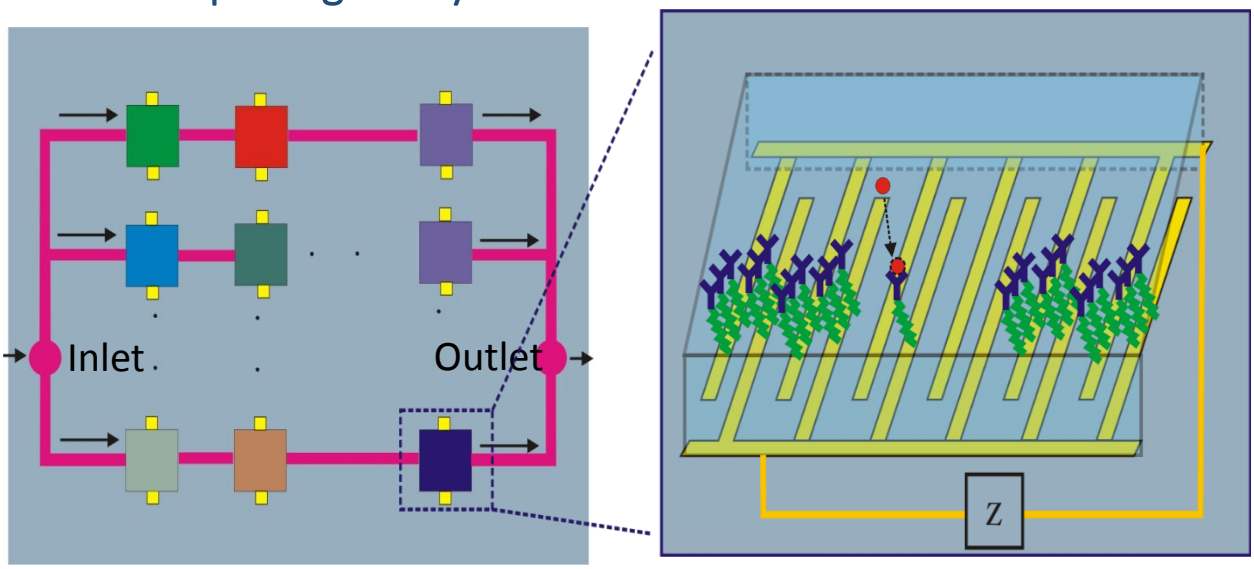

Figure 3: Representation of Multiplexing in Biosensors [9]

Multiplexing makes it possible for the biosensors to measure several analytes at the same time. Current advances in technology especially miniaturization of electronics has made it possible to do multiplexed measurements in biosensors.

The Figure 3 shows a block representation of a multiplexed measurement. Each colored pixel represents a set up to measure an analyte. Therefore if there m by n pixels, the product represents the total number of analytes the sensor is able to detect. The solution such as blood will flow through the inlet and out at the outlet such that it flows through each of the pixels. Presence of a specific analyte will be detected by the specific pixel for that analyte. Zooming in on a single pixel revels the channel and setup which is similar to the usual biosensor. Notice that each pixel requires a readout step. Carrying out the readout step for all of the pixels simultaneously will lead to a multiplexed measurement. The advantages of a multiplexed measurement would be that it saves time since it can make several measurements simultaneously.

1.3.4 Reproducibility and sensitivity

For a biosensor to be reliable and used to take tests such as point of care measurements for diseases then its results have to be reproducible. In which case repeating the same test should produce similar results at the readout step. On top of being reproducible, the biosensor should have a high sensitivity to the analyte to be determine. The sensitivity of a biosensor can be defined as the minimum

concentration of the analyte that can be determined. The lower the concentration, the more sensitive the biosensor is. The biosensor has to be sensitive since some analytes can be of low concentration in solution but whose concentration still needs to be determined. Therefore a highly sensitive biosensor will be required in such cases. On the other hand, some analytes can be of high concentration in solution and in such cases sensitivity of the biosensor is not as important.

1.3.5 Precision vs accuracy of readout technique

Precision is related to the ability of the system to measure changes in a characteristic such as impedance in the case of impedimetric biosensors while accuracy is related how accurate the measured characteristic is. For clinical biosensor applications accuracy as well as precision are important because the work of the sensor is to detect the absolute concentration of the analyte dependent on the accuracy small changes in bio properties also dependent on the precision. Therefore in this thesis we will concentrate in having as good an accuracy and precision as possible.

1.4 Point of Care Testing

When a patient visits a health center such as a clinic, the physician's office or a hospital they require a quick diagnostic of what might be wrong such as what might be causing the ailment. The problem with most current doctor visits today is that the patient will have to leave blood samples and then wait a couple of days or so to have tests carried out after which they can return to the doctor to get an interpretation of the results and a way forward such as possible treatments. The problem with this approach is the time commitment and need to wait for the results. With a point of care test approach the patient will visit the physician and after a brief interview, the physician can recommend possible quick tests to determine the problem. These tests can be carried out immediately (say within 20 min or so) at the medical center. Using the results a treatment can be devised for the patient and possibility of subsequent tests that may or not take longer. The advantage with point of care testing is that there is a reduction in the patient doctor visits with the tests being carried on the first visit and results interpreted immediately. It is no wonder that research in biosensors has pushed the development of these biosensors. In order to allow for the ability of point of care testing the biosensor should allow for several characteristics such as the following:

- System Portability to allow for easy testing even at smaller health centers
- Low cost systems mean that tests can be carried out on patients and the point of care sensors can be disposed of.
- The test time should be short to reduce the number of patient physician visits. For example the test and its interpretation can be carried out on the same physician visit.
- Low sample volumes are also a key characteristic for a point of care test in order to avoid phlebotomy, therefore the biosensor has to have good sensitivity.

On top of the characteristics mentioned above, point of care testing requires that the biosensors used meet the characteristics of general biosensors such repeatability and sensitivity. The electrical approach meets most requirements of a point of care testing approach due to the advantages it provides over the other approaches. This thesis explores the possibility of using electrical biosensors for point of care testing especially with the use electrical readout techniques. Electrical biosensors may not be so sensitive but possess other important characteristics such as easy to multiplex, differential measurement, low cost and portable. Note also that for point of care testing high sensitivity may not be of high importance since they are usually used by the physician to get a fast understanding of what might be wrong with the patient and not as final results.

1.5 Electrical biosensors

Due to advantages of electrical biosensors for point of care testing we have pursued an electrical approach for our biosensor system. Electrical biosensors can further be divided into several sub-groups according to the electrical method used by the transducer. These methods include:

I. Potentiometry. The potentiometric biosensor involves measurement of the potential difference between an indicator and a reference electrode or two reference electrodes separated by a permselective membrane. This potential difference is proportional to the logarithm of the ion activity (or concentration) [1].

II. Voltammetry. This method is based on measurement of a voltage. This method is commonly used in industry application such as in pH sensor systems.

III. Amperometry. This method is based on the measurement of a current that is a result of electrochemical oxidation or reduction of an electroactive species. The test is performed at a constant potential difference of the working electrode (Which is usually made of Platinum, Gold, or Copper) with respect to the reference electrode. Measuring currents in range of several nano-Amperes to micro-Amperes will be proportional to the concentration of the analyte [1].

IV. Impedimetry. This method measures the solution impedance when a small AC signal is applied at the interface with a constant DC offset. These measurements can be done for variable frequencies of the input AC signal and an Impedance spectrum plotted. The approach is thus termed as electrochemical impedance spectroscopy. When the bio-molecule gets attached to the bio-recognition element, then the impedance at the interface changes and this change can be used to detect the bio-molecule/target molecule.

Approach	Sensitivity	Usage	Multiplexing	Time	Issues
Impedimetry	Usually in range of $\mu g/mL$ For impedance spectroscopy	Not as common	Easily available such as 32 sensors in [10]	20-40 minutes	Mainly in sensitivity
Amperometry	Variable such as ng/mL to pg/mL in the Field effect sensor and pg/mL in the Electrochemical sensor	Available commercially	Possible but not as good as the impedimetric method	20-40 minutes for Field effect sensor and about 50-60 minutes for Electrochemical sensor [11]	Transport limitation is problematic in the field effect biosensor [11]
Voltammetry	___	Common in industry such as pH sensors	___	___	Limited applications
Potentiometry	Can achieve up to pg/mL	Available	Possible and similar to the impedimetric techniques	___	___

Table 1: Comparison of possible Electric biosensors

For applications in the medical field for point of care testing we selected the impedimetric biosensor that works by measuring impedance changes resulting from the addition of the analyte. The other possible approach would have been the amperometric using the electrochemical biosensor but this is time-limited since it takes 50-60 minutes. With increased research interest in impedimetric biosensors and biosensor readout techniques we chose to explore this promising field of research for a point of care testing application [12].

1.6 Impedimetric Biosensor

Due to the availability of complex semiconductor fabrication techniques, microfluidics can be integrated in silicon processes enabling the complex integration of biosensors and the readout step. Such techniques have led to a lot of research on impedimetric biosensors [12]. From the description in the previous section these biosensors determine the concentration of the analyte by measuring a change in impedance of the sensor that results from the binding of the analyte usually an antigen with the bio-recognition element which is usually an anti-body. This impedance can be determined using electrical techniques. The advantage that the impedimetric biosensor has is easy integration with silicon processes, a simple electrical model and the ability to meet the characteristics of biosensors. The impedimetric biosensor can meet many of the characteristics of biosensors if not all. For example they can easily meet the multiplexing ability by using analog switches to select which sensor (channel) to read out, a differential measurement can be carried out by subtracting two electrical signals resulting from two sensors. The other advantages are the portability of electrical readout techniques and also it is possible to mass produce low cost electrical version of the sensor that can be used for point of care testing. The rest of this section will describe an impedance based model for an impedimetric biosensor.

1.6.1 Model of an Impedimetric biosensor

In this section we will see an electrical analogy of the impedimetric biosensor. Using this electrical model and its electrical characteristics we can use its electrical properties to analyze the effect the addition and binding of the analyte has on the sensor's electrical properties

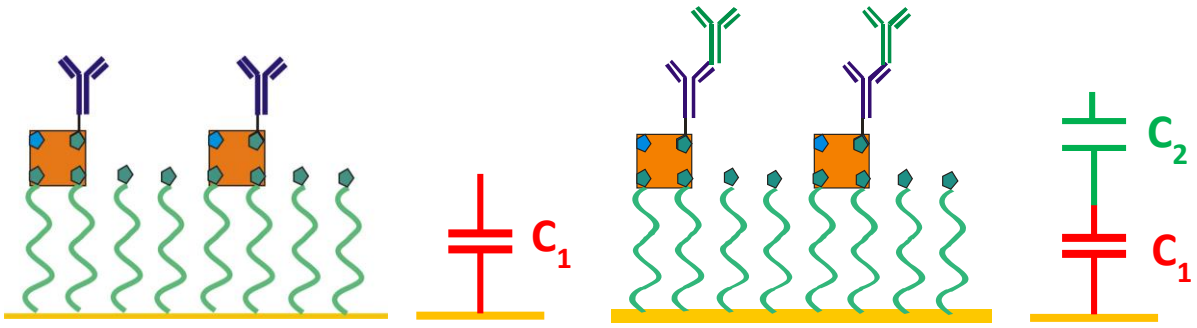

Figure 4: General Model of Impedimetric biosensor

From the figure above we see a general model of the impedimetric biosensor. The first stage shows the sensor before the analyte is added. It consists of a gold surface to which the S Adenosyl methionine (SAM) is added. The SAM plays a role of separating the antibody from the gold plate and hence preventing any interaction between the antigen (analyte to be tested) with the gold plate. Then Streptavidin (SA) is added which binds with the SAM and enables the binding of the antibody. Next the antibody is added to the channel and forms a bond on the SA. At this point the sensor is complete and ready to use. The sensor can be modelled by the circuit diagram below

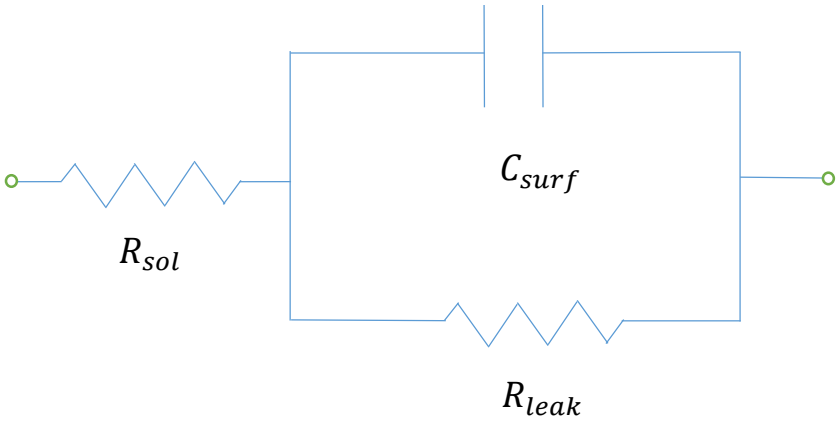

Figure 5: Circuit Schematic of an Impedimetric Biosensor [10]

From the above circuit, the Impedimetric biosensor can be modelled using an equivalent circuit of capacitors and resistors. R_{Sol} is a small series resistance that results from ions drifting in the solution bulk in response to an applied voltage. This is usually a constant resistance that can be predicted but is typically left as a fitting parameter [10]. The leakage resistance R_{leak} is a high impedance in parallel with the surface capacitance which is usually infinite if no redox species are present but in practice it is finite [10]. C_{surf} is a series combination of the surface modulation capacitance and the ionic double layer capacitance of the biosensor as the solution consisting of the bio recognition element and the SAM form a dielectric on the conductive gold plates. The surface modulation capacitance can be modelled as a dielectric capacitance that is given as $c = \frac{\varepsilon A}{d}$ where ε is the permeability of the membrane and d is the dielectric constant. In the figure above it is shown as C1. When the bio-molecule to be detected is bound on the bio-recognition molecule the series double layer capacitance changes as shown in a new series capacitance C2.

To demonstrate the impedance of a biosensor we use typical values for a modelled impedimetric biosensor. For example consider $R_{leak} = 1M\Omega$, $C_{surf} = 30nF$ and $R_{sol} = 400\Omega$, which are extracted values for these circuit elements obtained from the impedimetric biosensor in [10].We can then determine the impedance of a general biosensor system as below

$$Z_s = R_{Sol} + Z_{surf} || Z_{leak}$$

$$= R_{Sol} + \frac{R_{leak}}{R_{leak} C_{surf} s + 1}$$

Substituting in the typical values above we can then determine the impedance versus frequency for this specific biosensor model and a plot is plotted below.

The Figure 6 and Figure 7 below show how the impedance of a typical impedimetric biosensor varies with frequency. From the figures we see three distinct regions where one of the elements dominates the total impedance. At low frequencies the impedance is dominated by the $R_{leak}$the leakage resistance of the biosensor shown in the low frequency plateau. The phase plot in this region also shows the phase being low or near zero corresponding to the impedance being dominated by a resistive impedance. Increasing the frequency leads to reduction of the capacitive impedance until its impedance is lower than that of the leakage resistance, at which point the impedance is dominated by the capacitor. Comparing with the phase plot we see that phase is approaching -90^o (specifically the phase is in the range of -80^o) which is because capacitive impedance is now dominating in this region. Further

increasing the frequency will reduce the capacitive impedance until the net impedance is dominated by the R_{sol} shown in region 3. The phase in this region also approaches zero because the resistor is dominating the net impedance at this frequency region.

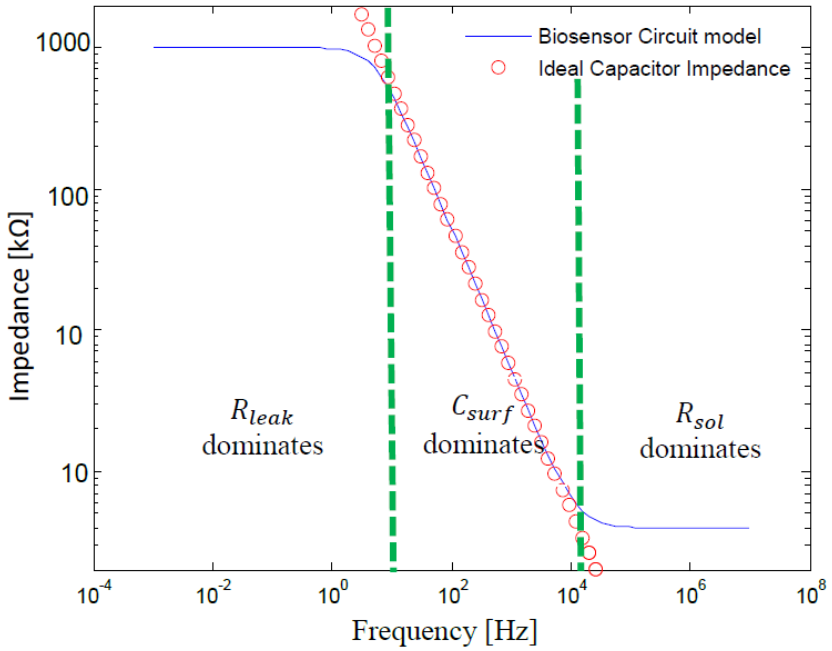

Figure 6: Magnitude plot for a typical biosensor

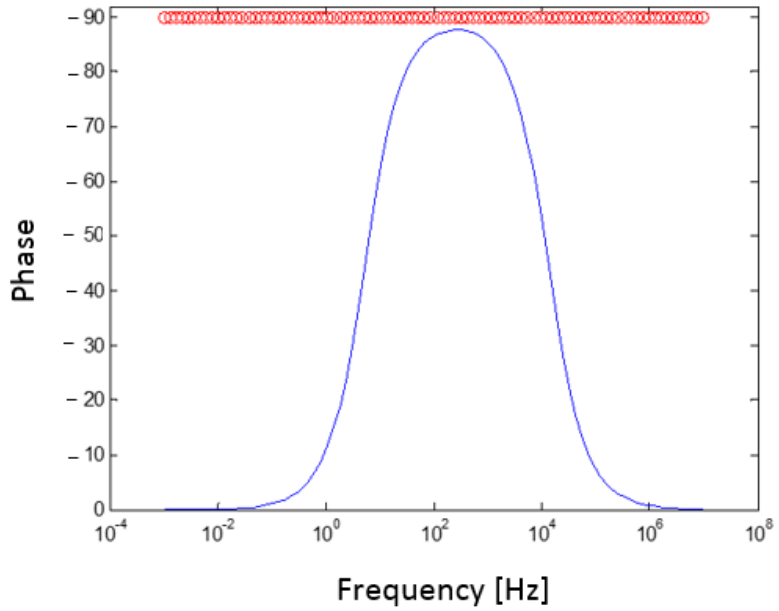

Figure 7: Phase plot for a typical biosensor

Therefore appropriate choice of a measurement frequency will approximate the impedance as a capacitor. This is the frequency range we prefer to make measurement in because addition of the antigen will change the surface capacitance as shown above. Ignoring the apparent effect of the resistances in the model will simplify the readout and post-readout processing of the electrical signals.

From the magnitude and phase plots above, this range is determined to be between 1 KHz-30 KHz for many impedimetric biosensors.

1.6.2 Electrical Readout

Now that the model of the biosensor is determined, the problem boils down to an impedance measurement set up for the readout. The challenge is to develop an electrical impedance meter that can measure the impedance of the sensor with varying frequency. One quick solution to this problem would be to purchase a standard impedance analyzer such as those developed by Agilent. This solution will give an accurate measurement for the impedance in the frequency range required. The problem this solution presents is that impedance analyzers are usually bulky and also expensive. Also because the impedance analyzer is an already complete built system, it does not permit easy access to the electronics inside it in case any modifications are required and this causes problems in case we want to do a multiplexed measurement or even differential measurements. The combination of these problems eliminates the impedance analyzer as a possible solution. A possible solution could be a board level design consisting of embedded electronics whose connection can be controlled however the user (or designer) wishes. Better still a solution could involve completely integrating the electronics with the biosensor as demonstrated in [10].

Some electrical techniques to measure impedance are described below.

Bridge Method

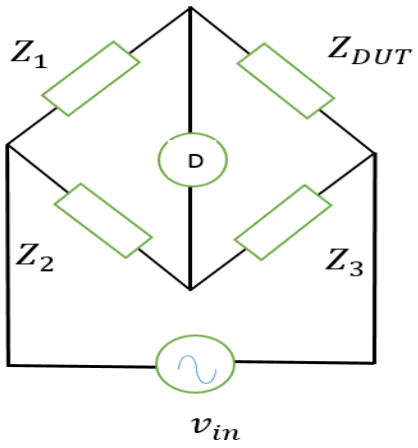

Figure 8: Schematic of the bridge method based on [13]

This method involved determination of a variable impedance using know impedances (usually 3) in a bridge configuration. By varying one of a combination of the impedances, the bridge can be balanced such that no current goes through a galvanometer D in the middle of the bridge as shown in Figure 8. The Impedance under test can then be determined when no current is flowing through the detector as a ratio of the other known impedances. The Device under Test (DUT) can be determined as

$$Z_{DUT} = \left(\frac{Z_1}{Z_2}\right) Z_3$$

Z_1, Z_2 and Z_3 can be chosen as combinations of resistors, inductors and capacitors depending on the form of the impedance being measured. For example measuring a capacitive impedance we could use Z_1 and Z_2 as resistors and Z_3 as a variable capacitor that can be tuned to balance the bridge. This method is highly accurate since it only requires sensing of zero current. A problem with this method is that it is typically manually operated to set the zero point for the current detector. This affects the accuracy if a changing impedance (or time varying impedance) is used.

Resonant Method

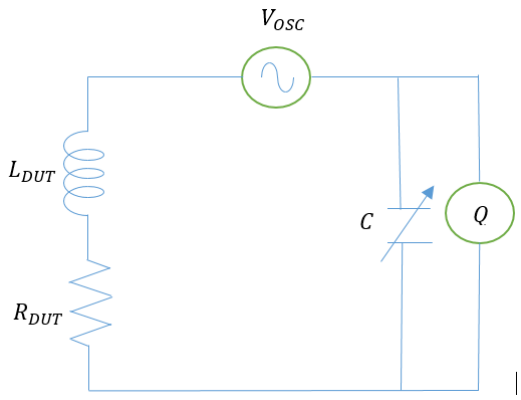

Figure 9: Circuit Schematic of the Resonant Method [13]

Figure 9 shows the schematic for the resonant method for impedance determination. In the circuit above the impedance to be determined is a series inductor and resistor combination. The circuit above is adjusted to resonance by tuning the value of the capacitor C. Then the value of L_{DUT} and R_{DUT} can be determined from the Frequency of V_{OSC} , C and the quality factor Q of the circuit. For different impedance measurements different connections can be used such as the series or parallel connection. The disadvantages with this approach is that the circuit has to be connected differently depending on the impedance being measured and also the fact that we manually need to tune the value of C to determine the impedance. Also most tuned capacitor values are hard to determine precisely affecting the accuracy of the measurement.

IV Method

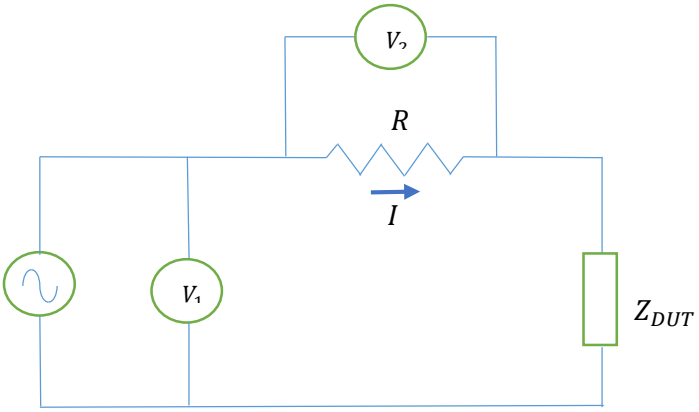

Figure 10: Circuit Schematic of the I-V Method [13]

Figure 10 shows the circuit schematic of the I-V method to determine an unknown impedance. This method works by measuring the voltage across the DUT and then the current through it. The impedance can then be determined by the ratio of these two parameters. The voltage can be measured directly and the current measured by measuring the voltage V_2 across a known small series resistance. Then:

$$Z_{DUT} = \frac{V_1}{I} = \frac{V_1}{V_2} R$$

The disadvantage with this method is that it doesn't consider the voltage drop across the small resistor R and therefore it is intrinsically inaccurate. According to [13] one method to improve the accuracy of this method is to use a transformer to replace R. In this case the primary of a transformer would be in place of the resistor and the secondary used to measure the current through the transformer. A clear disadvantage with this new approach (when a transformer is used) would be the inability to measure impedances at low frequencies or at DC measurements because the transformer only works for alternating current signals.

Auto-balancing bridge Method

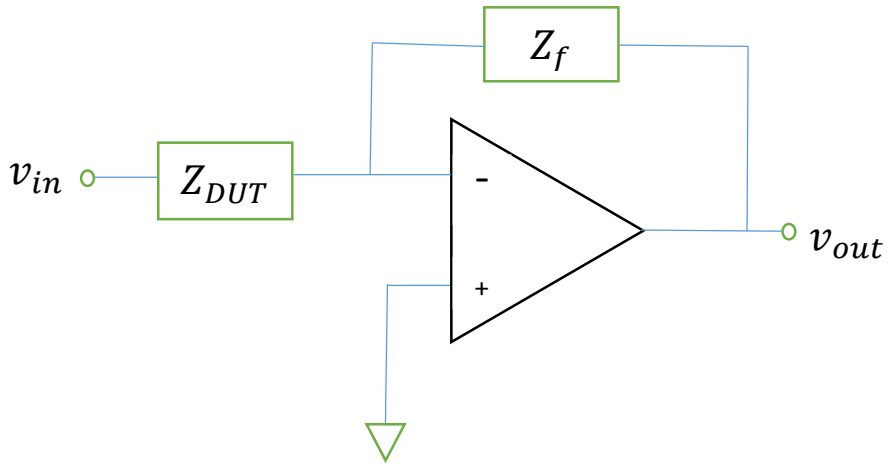

Figure 11: Circuit Schematic of the Auto-balancing bridge Method [13]

Figure 11 shows a simple schematic of an impedance meter circuitry using the auto-balancing bridge method. The input to the impedance meter is an AC voltage. When this voltage drives the impedance under test Z_{DUT} a current is produced. This current is then converted to a voltage by the feedback impedance Z_f. Knowing the feedback impedance Z_f , the input voltage v_{in} and measuring the output voltage v_{out} can determine the value of the Z_{DUT}. Below is a simple mathematically equations explaining this thought process.

$$i_{dut} = \frac{v_{in}}{Z_{DUT}}$$

$$v_{out} = i_{dut}(Z_f)$$

$$= -\left(\frac{Z_f}{Z_{DUT}}\right) v_{in}$$

$$Therefore\ Z_{DUT} = -\left(\frac{v_{in}}{v_{out,DUT}}\right)Z_f$$

A challenge with this approach is the need to measure both the input and output voltages. This can be avoided by doing a ratiometric measurement. With this measurement, another impedance whose magnitude and phase variation is placed in the place of the Impedance under test and its output voltage is measured as a response to the same input voltage. Then we know that

$$Z_{CAL} = -\left(\frac{v_{in}}{v_{out,CAL}}\right)Z_f$$

We can then obtain a ratio of Z_{DUT} and Z_{CAL} by dividing the equations above to get

$$\frac{Z_{DUT}}{Z_{CAL}} = \frac{v_{out,CAL}}{v_{out,DUT}}$$

Therefore knowing the value of Z_{CAL} we can obtain a value for Z_{DUT} as

$$Z_{DUT} = \left(\frac{v_{out,CAL}}{v_{out,DUT}}\right)Z_{CAL}$$

The above is a simpler problem to solve that the previous case where we had to measure the input voltage as well.

The advantage this method has is that it is relatively accurate for frequencies below 1 MHz, which is where many biosensors are operated. The other and critical advantage is that the ability for automated measurement without the need to tune the circuitry hence making speedy impedance measurement over time. Note though that proper choice of Z_{CAL} is required to have a good accuracy and minimize measurement error.

Therefore to do an impedimetric biosensor we used the same ideas as in the auto-balancing bridge method. The idea of a generic impedance meter can be applied to the impedimetric biosensor. The biosensor can be placed as the impedance under test and its response to the AC input measured. A ratiometric measurement is then made with a calibration impedance Z_{CAL} after which we can determine the impedance of the biosensor [13].

1.7 Previous work on Impedimetric Biosensors

In this section we describe available systems that aid impedance measurement for electric biosensors. Some of the systems have been developed commercially while many others have been developed as part of an academic research.

I. The AD5933. This is an impedance measurement chip developed by Analog devices. This is a complete integrated impedance measurement setup that uses DFT Analysis to determine an impedance measurement. This system has some impediments for the specific application of impedimetric biosensors. The minimum AC output voltage of the system is 100mV, whereas many impedimetric biosensors have a peak-to-peak AC requirement of 10 $mV_{pp.}$ This can easily be overcome by using an attenuator circuit, in which case the accuracy might be reduced. Another disadvantage is that this system is difficult to work with since a lot of the systems are already customized for specific applications and therefore for other applications the system might be difficult working with. If the biosensor might require multiplexing, the AD5933 does not easily support this feature and would require external analog switches that would be difficult to interface with the chip. System accuracy for

the AD5933 is also limited to 0.5% and for systems requiring accuracy of more than this value it would require another system.

II. The Agilent 4294A Precision Impedance Analyzer, which measures impedances from the range of 40Hz-110MHz. The accuracy of the system is up to 0.1% which is good. The major issue with the impedance analyzer is that it costs about $30000, which is too expensive for point of care testing. Another issue is the size; the Agilent 4294A is bulky again affecting its ability to work in a point of care application. Finally, since the Agilent 4294 is an already complete black box system, it is difficult to integrate other functions such as multiplexed measurements.

III. Lock-in technique for complex impedance measurement. Another method for complex impedance measurement used in [14] is based on the lock-in technique for measuring the real and imaginary part of an impedance. The readout technique is based on a system related to the auto-balancing bridge method with the use of analog demodulation techniques to determine the real and imaginary part of the measured impedance. This system is able to do a real time impedance measurement, a multiplexed and differential measurement for several sensors with currents as low as several nana amperes. The system also uses the input source as a reference to the demodulator. This means the accuracy of the system depends on how accurately we can determine the input voltage. The demodulator circuitry can also result in extra noise in the system. For this system the fact the different sensors go through different paths such the amplification and demodulation, can result in measurement errors and high power consumption of the system. The system is able to measure accuracy of 0.5% for a 1nF capacitor as described in [14].

IV. Another system described in [10] uses a ratiometric measurement to determine the measured impedance. This system has two paths for measurement. The first path is the calibration path and the other path is DUT path. The calibration path uses a known calibration impedance and the DUT path is used for the unknown impedances. The system was able to multiplex 32 DUTs and achieve a precision of 0.2% on an IC design of the readout system. One limitation of this setup was the use of two different paths for the calibration and DUT steps.

1.8 Chapter Conclusion and Thesis Organization

With the increase in need of point of care testing the need for biosensors has increased tremendously. Therefore biosensors that meet the characteristics described in this chapter are becoming desirable especially in the medical industry. Characteristics such as multiplexing to enable several tests to be carried out simultaneously, differential measurement to enable high sensitivity testing are driving research in biosensors. These characteristics can be met easily using electric readout techniques and therefore the increased research in this area. In this chapter we saw the advantage that electrical readout techniques provide such as cost saving and portability.

We then compared the possible electronic methods to readout the signals from the biosensor by measuring an impedance (particularly a capacitance or resistance). The method that was selected for our particular biosensor, which operates in the range 1 kHz-30 KHz as a capacitor, was the auto-balancing bridge method because of its good accuracy in this frequency range and ability to allow for a simple and quick readout.

Chapter 2 will then describe in detail this electrical readout technique based on the MAX32600 which is an embedded system by Maxim Integrated with an analog front-end. It will further describe how this system achieves the characteristic necessary to allow point of care testing such as the cost, device portability and ease of use in tests. Multiplexing ability and the ability of this system to do a differential method are also examined here. In this chapter we also describe how the feedback impedance and

calibration impedance are chosen in order to improve the accuracy of the system. A noise analysis is also made to determine how noise in the circuit affects the accuracy of the measurement setup

Chapter 3 describes the tests to determine the accuracy and precision of the readout technique using the MAX32600 board. Measurements are made of known impedances such as combinations of capacitors and resistors against the values obtained from an impedance analyzer at high accuracy. Next a complete protein measurement setup is measured using this setup and a comparison is made with a similar measurement using an impedance analyzer. The multiplexing and differential measurement ability of the board is also shown here.

Finally chapter 4 describes the future areas of improvement for example how to achieve more multiplexing ability. The milestones of this set up are described here including an approach to choosing the calibration impedance and the feedback impedance depending on the impedance to be measured.

Chapter 2: Impedance Measurement System

This chapter describes the general impedance measurement circuitry based on the MAX32600. The system describes the circuitry used, first explaining the choice of circuit variables such as the feedback impedance in the measurement circuit and the choice of the calibration impedance as well. Next we describe sources of measurement error in the system such as the effect of the amplifier Gain Bandwidth Product (GBP), noise sources in the system, and the switch resistance of the onboard analog Single Push Single Throw (SPST) switches. All these error sources are accounted for and their effect on the measured impedance is determined. Steps to overcome measurement errors from these sources are then determined and taken for example we recommend using high bandwidth op amps (or transimpedance amplifiers), describe calibrating the system for the switch resistance of the SPST switches, and also describe the use of averaging the measured output to overcome output noise.

2.1 System Description

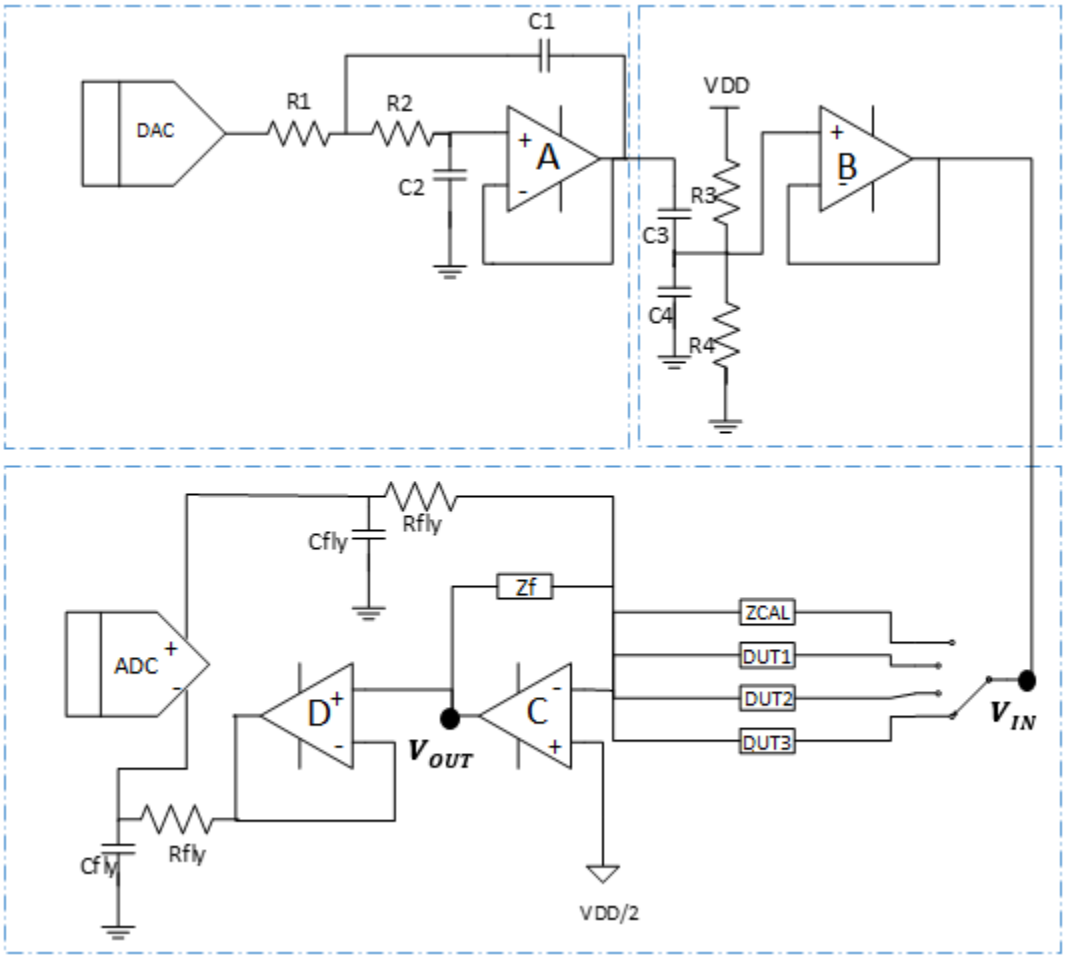

Figure 12: Circuit Schematic of the Entire Impedance Measurement setup

The Figure 12 shows the general Impedance meter schematic. The Impedance measurement setup can be broken down into three main parts as shown in the schematic above and described below.

I. The signal creation stage that consists of a DAC and a low pass filter

II. The Attenuator to decrease the amplitude of the sinusoid
III. The Measurement stage of the impedance

These three stages are described further below.

2.1.1 Signal Generation Stage

The DAC is used to produce a sinusoid at a given frequency. The DAC used is a 12 bit DAC on the MAX32600 Evaluation Board. The DAC is set to a reference voltage of 1.024V and the peak to peak output is set to 100mV. The next part of the first stage consists of a Sallen-Key low-pass filter that removes the high frequency elements from the DAC output to produce a cleaner sinusoid. R_1, R_2, C_1, C_2 are chosen to set the cut-off frequency for the second-order low-pass filter. The transfer function $H(s)$ for the low-pass filter can be obtained as

$$H(s) = \frac{{\omega_0}^2}{s^2 + 2\alpha s + {\omega_0}^2}$$

$$\text{Where } \omega_o = 2\pi f_0 = \frac{1}{\sqrt{R_1 R_2 C_1 C_2}} \text{ and } \alpha = \frac{1}{C_1}\left(\frac{R_1 + R_2}{R_1 R_2}\right)$$

And f_0 is the undamped natural frequency of the filter. A choice of f_0 can be made depending on the frequency range of the input sinusoid so that high-frequency components from the DAC output will be filtered out. For example for this set-up we chose $R_1 = 200K\Omega, R_2 = 200K\Omega, C_1 = 68pF \; and \; C_2 = 11pF$. Then $f_0 = \frac{1}{2\pi\sqrt{R_1 R_2 C_1 C_2}} =$ 29 KHz.

2.1.2 Attenuation Stage

After the filter stage is an AC attenuator. Because of the sensor requirements we require an AC signal that is less than $10mV_{pp}$, therefore an attenuation stage is required. The attenuator is set by capacitors $C_3 \; and \; C_4$ and the attenuation factor can be given as $\frac{C_3}{C_3 + C_4}$. Because of the current limit of the op amp A at the output, $C_3 \; and \; C_4$ are chosen so that the maximum AC current through these capacitors doesn't exceed the short-circuit current at the op amp output given by I_{SC}. The maximum current through the capacitors at a given frequency is given by

$$I_{max} = V_{max} C_a \omega$$

Where:

- V_{max} is the maximum voltage output from the low pass filter from op amp
- C_a is the series combination of capacitors $C_3 \; and \; C_4$ given by $C_a = \frac{C_3 C_4}{C_3 + C_4}$
- And ω is the angular frequency of the driving sinusoid

This current becomes larger at higher frequencies as shown by the equation above. Therefore we can obtain the maximum possible current through the attenuator capacitors knowing the maximum frequency of the driving sinusoid. For our application, the maximum operating frequency can be up-to 50 KHz and $V_{max} = 5mV$. Assuming $C_3 = 1nF \; and \; C_4 = 10nF$, therefore $I_{max} = 1.4mA$. This value is below the I_{SC} of the op amp A and therefore a good choice for $C_3 \; and \; C_4$.

The Resistors R_3 and R_4 can be chosen to set the DC voltage of the AC drive to the DUT. For our application this level is chosen to be $\frac{V_{DD}}{2}$, half the supply voltage, to increase the AC swing at the output of the last gain stage. Therefore we set $R_3 = R_4$. Care also has to be taken when choosing the values of

R_3 and R_4 considering $C_3\ and\ C_4$ so that the time constant is not too long to allow the DC level of the attenuator to settle down to $\frac{V_{DD}}{2}$.

The follower op amp in the end of this stage is used to provide an infinite input impedance to the attenuator so that the attenuated voltage is not affected by the value of the DUT.

2.1.3 Measurement Stage

After the attenuation stage is the actual measurement for the DUT. From Figure 12, the switches S1-S4 are used to perform a multiplexed measurement. In our system 4 measurements can be made, one for a calibration impedance and three for actual DUTs. Knowing the value of the calibration impedance, the output voltage from the third op amp in the schematic for each of the impedances we can obtain the value of each of the impedances.

Suppose the output at op amp C is $Y(s)$, and $X(s)$ is the input just after the op amp B (output of op amp B), then we have that

$$Y_{CAL}(s) = \left(\frac{-Z_{fb}}{Z_{cal}}\right) X(s) \text{ and then}$$

$$Y_{Z_i}(s) = \left(\frac{-Z_{fb}}{Z_i}\right) X(s) \text{ Where } Z_i \text{ represents the impedance i for i=1, 2, 3 for each DUT.}$$

$$\frac{Y_{CAL}(s)}{Y_{Z_i}(s)} = \frac{\left(\frac{-Z_{fb}}{Z_{cal}}\right)X(s)}{\left(\frac{-Z_{fb}}{Z_i}\right)X(s)} = \frac{Z_i}{Z_{cal}}$$

And therefore we can obtain Z_i as,

$$Z_i = \frac{Y_{CAL}(s)}{Y_{Z_i}(s)} Z_{cal}$$

Knowing the exact value of Z_{cal} and measuring $Y_{CAL}(s)\ and\ Y_{Z_i}(s)$ we can obtain the value of the impedance Z_i.

To accurately measure the value of Z_i we need to optimize the choice of Z_{cal} and Z_{fb} so as to maximize the signal-to-noise ratio (SNR). The steps to optimize these variables are explained further in this chapter.

The next stage is conversion to a digital signal using the ADC. Before the output of the last stage op amp is input to the ADC, a low-pass filter consisting of $C_{fly}\ and\ R_{fly}$ is applied to it. This filter helps absorb the charge injected back to the input of the ADC when the switch to the ADC turns off. The series resistance helps maintain the stability of the op amp when driving a capacitive load. The ADC will receive an analog signal and convert it to a digital signal that can be processed by the microcontroller code. For the MAX32600, the system uses a 16 bit ADC for this step with a programmable gain array (PGA) that provides variable gains of 1, 2, 4, and 8 depending on the need.

The final part is to determine the magnitude and phase of the output voltage, and signal processing to calculate the measured impedance. There are several methods that can be used to determine the magnitude and phase of the output voltage. These methods are listed below.

I. Fast Fourier Transform. This method is the most common one. The disadvantage of using the FFT is that it requires many samples, hence making it a power-hungry method. Therefore in instances where saving power is important the FFT should be avoided.

II. Analog down-conversion. This method uses parallel analog channels which are susceptible to channel mismatch induced performance degradation [15].

III. Quadrature Amplitude Multiplexing (Q.A.M). This method samples the output sinusoid at four times its frequency. These four samples can be used to obtain a value for the magnitude and phase. To improve accuracy and precision, more samples can be obtained and then averaged. Because few samples are required this method is power-efficient when compared with the FFT method [15].

Because of the advantage it provides as a low-power method, Q.A.M was used to determine the magnitude and phase output to the ADC. Suppose $x(t)$ is the input and $y(t)$ the output, then below shows the mathematical analysis for Q.A.M.

For sinusoidal $x(t) = \cos(2\pi F_c t)$ then we have that $y(t) = V_G \cos(2\pi F_c t + \theta)$ where V_G is the voltage gain and θ is the phase shift of the output from the input. To determine the magnitude and phase of the output voltage $y(t)$ using quadrature amplitude multiplexing we can sample the output voltage at 4 times its frequency (which is the same as the input frequency). Sampling the output at this frequency, $4F_c$, we have the samples as

$$y(k) = V_G \cos\left(2\pi F_c \frac{k}{4F_c} + \theta\right) \text{ For k=0,1,2,3, …}$$

$$= V_G \cos\left(\frac{\pi}{2}k + \theta\right) \text{ For k=0,1,2,3, …}$$

And the substituting in k=0, 1, 2, 3, ... we have that

$$y(k) = V_G \left(\cos\left(\frac{\pi}{2} * 0 + \theta\right), \cos\left(\frac{\pi}{2} * 1 + \theta\right), \cos\left(\frac{\pi}{2} * 2 + \theta\right), \cos\left(\frac{\pi}{2} * 3 + \theta\right), \ldots\right)$$

$$= V_G(\cos(\theta), -\sin(\theta), -\cos(\theta), \sin(\theta), \ldots)$$

Using $V_G e^{j\theta} = V_G \cos(\theta) + jV_G \sin(\theta) = I + jQ$

Then $I = y(0)\ and\ Q = -y(1)$

Knowing $I\ and\ Q$ we can determine $V_G\ and\ \theta$ as

$$V_G = \sqrt{I^2 + Q^2} \text{ and}$$

$$\theta = \text{atan2}(Q, I)$$

With just two samples we can obtain the magnitude and phase of the output wave. To improve the accuracy and precision of the measurement we can average several samples of the output wave as shown below.

$$\hat{I} = \frac{2}{N+1} \sum_{i=0}^{\frac{N+1}{2}-1} y(2i) * -1^i$$

$$\hat{Q} = \frac{2}{N+1} \sum_{i=0}^{\frac{N+1}{2}-1} y(2i+1) * -1^{i+1}$$

Then

$$Phase = \theta = atan2(\hat{Q}, \hat{I})$$ And

$$Magnitude = V_G = \sqrt{\hat{I}^2 + \hat{Q}^2})$$

From the above mathematical derivations [15] we see that the respective samples will have a $\frac{\pi}{2}$ phase difference from each other. Knowing the first and second samples without a DC offset we are able to determine both the magnitude and the phase of the output. The first sample is I and the second sample is the Q term. To improve the accuracy, precision and noise suppression of the measurement an averaging of N samples is done. For this application, we used N=399, therefore we obtained 400 actual samples from the ADC. A differential measurement was done so as to eliminate any DC voltage that could have resulted from the DC offset of the op amps and parasitic components in the system.

2.2 Measuring Impedances

To optimize the accuracy and precision of the impedance meter, we need to optimize the choices of Z_{CAL} , Z_f , the operating frequency range and the op amp C choice. For the optimization to be good we also need to know the form of impedance that we are testing, Z_{DUT} for example if Z_{DUT} is a purely capacitive impedance, purely resistive impedance, a series combination of capacitive and resistive impedance or even a parallel combination of resistive and capacitive impedances. Knowing this will help to accurately determine the other variables.

Below we discuss how we can optimally choose each of these variable to optimize the entire system.

2.2.1 Choice of Z_f

Because the input voltage swing is low – less than 10 mV_{pp}, in order to optimize the SNR of the ADC we require some form of gain through the measurement stage. The next stage, a PGA, also improves of the SNR. For our application, this gain is set to 8, the maximum possible gain from the PGA. Knowing that the PGA gain is set to 8, the ADC full range, and the Z_{DUT} range, we can determine an optimal value for Z_f . First defining:

- V_{ADC} as the ADC full range voltage, which was set to 2048mV
- $V_{IN,pp}$ as the input sinusoidal peak to peak voltage, which is 10mV maximum
- K_{pga} as the gain of the PGA, set to 8

Then,

$$\left(\frac{-Z_f}{Z_{DUT}}\right) * V_{IN,pp} * K_{pga} \leq V_{ADC}$$

Substituting in known values we have that

$$\frac{|Z_f|}{|Z_{DUT}|} * 80 \leq 2048$$

$$\frac{|Z_f|}{|Z_{DUT}|} \leq 25.6\,.$$

Therefore the maximum possible gain from the first gain stage is 25.6. Now suppose that both $Z_{DUT}\ and\ Z_f$ are pure capacitors. Assuming also the maximum capacitance to be measured is 60nF, then to set Z_f as a capacitor we need $Z_f = \frac{1}{C_f s}$ and $Z_{DUT} = \frac{1}{C_{DUT} s}$

We have that $C_f > \frac{C_{DUT}}{25.6} = \frac{60}{25.6} nF = 2.344nF$.

We know that we cannot just have a capacitor by itself in the feedback path because no element is setting the DC voltage across it. Therefore we require a resistor, R_f, in parallel with the capacitor chosen. The addition of a parallel resistor also converts this stage into another filter stage. Below we consider some possible forms of Z_{DUT} and how this gain stage becomes a filter.

I. Purely resistive impedance.

For a purely resistive impedance, $Z_{DUT} = R_d$, and the closed-loop transfer function for the op amp D is

$$\frac{-R_f}{R_d(R_f C_f s+1)}$$

This is a first-order low-pass filter with $f_{3dB} = \frac{1}{2\pi R_f C_f}$. Therefore, appropriately choosing the 3dB point for this first-order low-pass filter by varying R_f, we can optimize the choice of Z_f. For example, if the frequency range for the measurement is from 500Hz-30 KHz, we can set the value of $f_{3dB} = 500$ and therefore determine $R_f = \frac{1}{2\pi f_{3dB} C_f}$. Using known values from above we have that $R_f = \frac{1}{2\pi * 500 * 2.344 * 10^{-9}} = 135.8K\Omega$.

II. Purely Capacitive Impedance.

For a purely capacitive impedance, $Z_{DUT} = \frac{1}{C_d s}$, and the closed-loop transfer function for the op amp D is

$$\frac{-R_f C_d s}{(R_f C_f s+1)}$$

This is a band-pass filter with upper 3dB point $f_{3dB,u} = \frac{1}{2\pi R_f C_f}$. Again, appropriately choosing this point will eliminate the high-frequency noise. One choice for the $f_{3dB,u}$ can be as above in the purely resistive case, setting $R_f = 135.8K\Omega$.

III. Parallel Capacitor and Resistor.

For a parallel capacitor and resistor combination, $Z_{DUT} = \frac{R_d}{(R_d C_d+1)}$, and the closed-loop transfer function for the op amp D is therefore given as

$$\frac{-R_f}{R_d}\left(\frac{R_d C_d s + 1}{R_f C_f s + 1}\right)$$

In case if $R_d C_d < R_f C_f$, then this is a band-pass filter with lower 3dB point $f_{3dB,l} = \frac{1}{2\pi R_d C_d}$ and upper 3dB point $f_{3dB,u} = \frac{1}{2\pi R_f C_f}$. Again, appropriately choosing this point will eliminate the high-frequency noise. One choice for the $f_{3dB,u}$ can be as above in the purely resistive case, setting $R_f = 135.8K\Omega$.

IV. Series Capacitor and Resistor

For a series capacitor and resistor combination, $Z_{DUT} = \frac{R_d C_d s+1}{C_d s}$, and the closed-loop transfer function for the op amp D is given as

$$\frac{-R_f C_d s}{(R_f C_f s + 1)(R_d C_d s + 1)}$$

Suppose that the DUT is a capacitor with a small series resistance and then $R_d C_d s \ll 1$ for the frequency range of interest, then we have that

$$\frac{-R_f C_d s}{(R_f C_f s + 1)(R_d C_d s + 1)} \approx \frac{-R_f C_d s}{(R_f C_f s + 1)}$$

But in case we can't ignore the effect of the series resistance R_d, then we have a second-order filter system with a low-frequency pole at $f_{3dB,l} = \frac{1}{2\pi R_f C_f}$ and a high-frequency pole at $f_{3dB,u} = \frac{1}{2\pi R_d C_d}$.

2.2.2 Choice of Z_{CAL}

To choose the calibration impedance we need to be aware of the impedance we are measuring. For example, if we are measuring capacitive impedances then we require a calibration impedance that is more capacitive. Another consideration is the range of the impedance we are measuring. If we are measuring a capacitive impedance that has a capacitance in the range of 10-60nF, then the calibration impedance should be in this range as well to improve the accuracy. Generally the closer the calibration impedance to the DUT the more accurate the measurement of the DUT. For the setup to choose a calibration impedance the system is setup such as to measure a biosensor. Since the biosensor is capacitive in the range 500 Hz-30 kHz, a frequency sweep is range of 500Hz- 13.9 kHz for our system and curve fitting techniques (described in Chapter 3) are used estimate the DUT value. As will be described further, the measurement amplifier bandwidth and voltage noise have an effect on the measurement accuracy. Therefore to have a good accuracy we used an LT1805 that has an 85MHz Gain bandwidth product and 21nV/rtHz noise voltage. To improve the noise immunity of the system, the measured voltages are averaged for 400 samples. The effect of averaging on noise is discussed later in this chapter when we discuss noise and how it affects the system accuracy.

To estimate the accuracy and precision of the measurement system we used 3 ceramic capacitors of values 4.7nF, 22nF and 33nF. These values were chosen to model typical biosensors and the ceramic capacitors are used since they have a low equivalent series resistance so as to have a good quality factor. The values of these capacitors are determined by a pre-calibrated Agilent impedance analyzer that is accurate to 0.1% for the frequency range of 500 Hz-14 kHz. The input sinusoid to the impedance is set as $10mV_{pp}$. The impedance spectrum is obtained from the Agilent analyzer and using the bode plot we are able to extract the capacitance by linearization of the bode plot magnitude. This therefore means our system accuracy is also limited to this value. For our system the measurement precision is determined as how stable the system is when measuring a fixed impedance (capacitor for our test) and the accuracy is determined as how close the measured impedance is to that derived from the impedance analyzer. The test for choice of calibration capacitor is carried out for capacitors of 4.7nF, 6.8nF, 22nF, 33nF and 47nF. For each calibration capacitance we take measurements for 5060s which would correspond to 110 time points considering 46s per frequency sweep. Again the measurements are carried out for 32 frequency points in the range of 500 Hz -14 kHz with no specific distribution in the range (but spread out almost equally per 1 kHz frequency increase). Measurements for each frequency point would take about 1s and correspond to averaging of 400 samples taken from an ADC at the output. When the frequency spectrum is obtained, the capacitance is then estimated from the bode plot obtained. This whole process is repeated 110 times for the each capacitance measurement point. Over a frequency sweep and time measurement we have that

$$RMS\ Precision = \frac{\sigma(DUT)}{\mu(DUT)} * 100\%$$

$$Peak\ to\ Precision = \frac{\Delta_{pp}(DUT)}{\mu(DUT)} * 100\%$$

Where

$\sigma(DUT)$ is the standard deviation in the measurement of the DUT capacitance over the measurement time.

$\mu(DUT)$ is the mean of the DUT capacitance over measurement time.

$\Delta_{pp}(DUT)$ is the peak to peak value in the measured DUT capacitance over the measurement time.

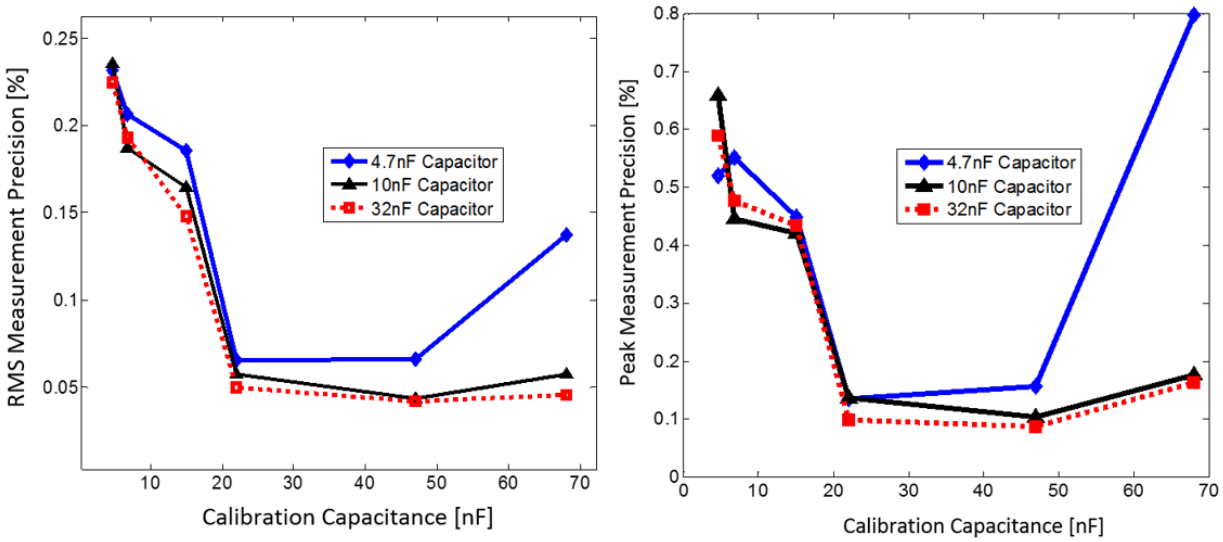

Figure 13: Plots Showing Precision Variation with Calibration Capacitance

Figure 13 shows the measurement precision defined as above when measuring 3 capacitors of value 4.7nF, 22nF and 33nF. For low values of the calibration capacitance the measurement error is high. The measurement error is high because of the low signal-to-noise ratio when a small calibration capacitor is used. Increasing the calibration capacitance increases the output signal hence increasing the signal to noise ratio. At high values of calibration capacitance, the large ratio between the calibration impedance and the measured capacitance (or impedance) increases the measurement error. Comparing the measured capacitor values to those obtained on the impedance analyzer for each of the capacitors we obtained the results shown below (for the calibration capacitor with the best precision).

Capacitance [nF]	Agilent Analyzer Value[nF]	MAX32600 system value [nF]	Accuracy relative to impedance analyzer [%]
4.7	4.9481	4.9652	0.344
10	10.7380	10.731	0.065
32	33.551	33.442	0.325

Table 2: System accuracy of MAX32600 relative to impedance analyzer

Because of the difficulty in determining accurately the calibration impedance (was determined to 0.1%) using the impedance analyzer, the accuracy of the measurement was almost independent of the value of the calibration impedance (specifically calibration capacitor) used but the lowest accuracy obtained was 1% of the value obtained from the impedance analyzer.

Another test to determine a choice for the calibration impedance is by comparing another choice for the calibration impedance such as using a calibration resistor to measure a capacitor. Using a 10KΩ resistor in the calibration path we measured both the RMS measurement precision and the peak to peak measurement precision. The RMS Measurement precision is 0.23% for 4.7nF Capacitor, 0.22% for a 10nF Capacitor and 0.21% for a 33nF Capacitor. The peak to peak measurement precision on the other hand is 2.22%, 2.15% and 2.04% respectively. From these values we see that to determine an impedance, we require that the calibration impedance be similar to the impedance being measured. The explanation for this trend could be related to the similar noise spectrum when the calibration impedance and DUT are similar. Repeatability of this measurement was shown when the measurement is repeated for the chosen calibration capacitor, where we obtained similar results.

2.2.3 Noise Analysis

Noise in the electronics is an important consideration that affects the accuracy and precision of the impedance measurement. There are several sources of noise (and interference) that we will discuss and these include:

I. Op amp input voltage and current noise. This is the noise at the terminals of the op amp. It can result from power supply noise, input op amp noise from the circuit model or the noise on the reference source that is used to set the DC reference for the op amp. This noise is modelled as a combination of voltage noise at the terminals of the op amp and a current noise at the same terminals.
II. Another class of noise source is the component-related noise. For example, resistors possess Thermal noise, which is also known as Johnson noise. For our measurement circuit, this noise source can be ignored since it is smaller than other sources due to the low resistance used and low bandwidth.
III. Electromagnetic interference (EMI) also affects the accuracy and precision. Several causes of EMI are associated with the layout of the printed circuit board (PCB) and addition of components to the PCB that create inductive loops on the board. Also, digital circuits on the circuit board are a source of EMI due to the handling of periodic waveforms and the fast clock/switching rates [16].

Noise Simulation

To see the effect the output noise has on the system we setup an LTspice simulation with the LT1805 op amp. The LT1805 op amp is the op amp used in the measurement stage shown in Figure 12 as op amp C. The choice of the LT1805 is due to the relative good bandwidth and low voltage noise rating. The circuit schematic for the measurement step is shown below. It is setup as external components on the prototyping matrix of the MAX32600 EvKit board.

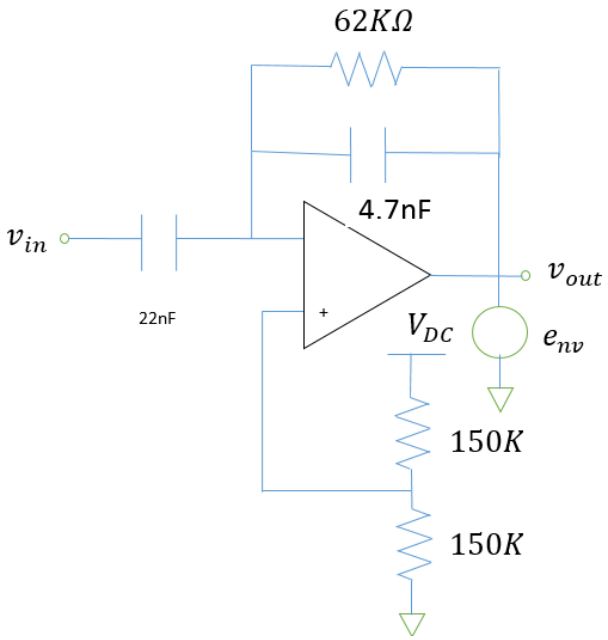

Figure 14: Circuit Schematic to determine Noise

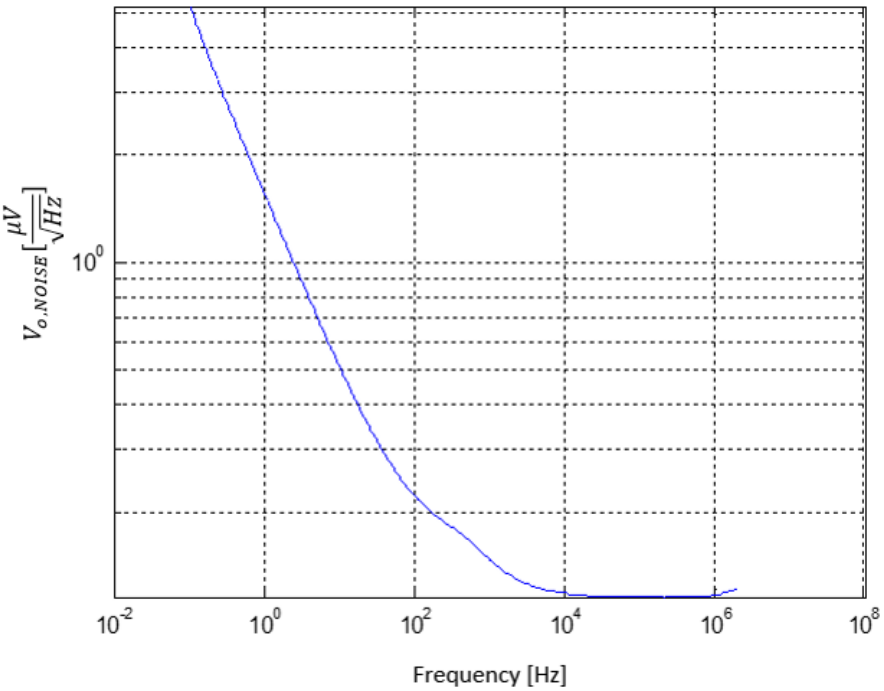

Figure 15: Output Noise variation with frequency for the setup

Figure 15 shows the output-referred noise variation with frequency for an input capacitor of 22nF. The output noise is composed of two components: at low frequencies (<10 kHz) it is dominated by $1/f$ noise, also known as flicker noise, whereas at higher frequencies (~10 kHz to ~100 kHz) it is constant

with frequency. To calculate the RMS noise voltage we can integrate over this noise curve. An estimate of the noise can also be obtained by determining these respective components and then using the formula for uncorrelated noise sources to obtain RMS voltage noise. The steps below show how a rough estimate can be obtained.

$$e_{nf} = efnorm * \left(\sqrt{ln\left(\frac{f_H}{f_L}\right)} \right)$$

where $efnorm$ is the noise voltage normalized at 1Hz, $f_L = 0.1Hz$ and f_H is the upper bandwidth of the circuit. f_L is usually set to 0.1 Hz for many op amp applications because not having a lower bandwidth limit for noise will lead to infinite noise for the system. f_H was set to 10 KHz from the bandwidth of the low pass filter input. Then we have that

$$e_{nf} = \frac{1.568\mu V}{\sqrt{Hz}} * \left(\sqrt{ln\left(\frac{10 * 10^3}{0.1}\right)} \right) = 5.32\mu V$$

$$e_{nBB} = e_{normBB} * \left(\sqrt{BW_n}\right)$$

Where e_{normBB} is the constant noise value with frequency and BW_n is the noise bandwidth given as $BW_n = 1.57 * BW$ for single-pole rollover and BW is the circuit bandwidth. $BW_n \approx 1.57 * (29.1 - 10)kHz = 30\ kHz$. Then

$$= \frac{0.12\mu V}{\sqrt{Hz}} * \left(\sqrt{30 * 10^3}\right) = 20.78\mu V$$

The RMS Noise can then be determined as

$$e_{nV} = \sqrt{{e_{nBB}}^2 + {e_{nf}}^2} = \sqrt{(20.78^2 + 5.32^2)}\mu V = 21.45\mu V.$$

Comparing the output noise with the input wave of 10mV, we can obtain the minimum signal-to-noise ratio for unity gain as

$$SNR = 20log_{10}\left(\frac{10}{.02145}\right) = 53.37dB$$

This SNR is low and corresponds to a measurement error of $\frac{21.45}{10*10^3} = 0.2145\%$ which may not be suitable for many biosensor applications. Therefore, to improve measurement accuracy and precision (this has an important effect on the precision), averaging the output voltage is used. In fact if we averaged the output voltage N times then we would reduce the output noise voltage by a factor of $\sqrt{N}$. For example for our case N=400, then we have that we are reducing the output noise voltage by a factor of $\sqrt{400} = 20$. In that case the overall circuit RMS noise is $\frac{e_{nV}}{20} = \frac{21.45\mu V}{20} = 1.073\mu V$. Then we have that

$$SNR = 20log_{10}\left(\frac{10}{.00173}\right) = 75.24dB$$

which is more than 20dB improvement in the previous SNR. The measurement error in this case can be estimated as $\frac{1.073}{10*10^3} = 0.011\%$. This is smaller than the obtained values from measuring different capacitors, where the system precision was ~0.1%. Therefore we can believe that op amp noise is not the largest cause of measurement inaccuracies in this system (at least with the choice of the op amp LT1805).

2.2.4 Op amp Bandwidth

The Bandwidth of the op amp will affect the accuracy of the impedance measurement. In Section 2.1.3 we described how the impedance measurement system works using a calibration impedance Z_f, feedback impedance Z_f and an op amp. The equations described in the setup were for an ideal op amp with infinite gain, but in reality op amps have finite gain, finite bandwidth and a phase response. Putting this into consideration we consider the actual gain equation for the impedance measurement setup in Figure 16.

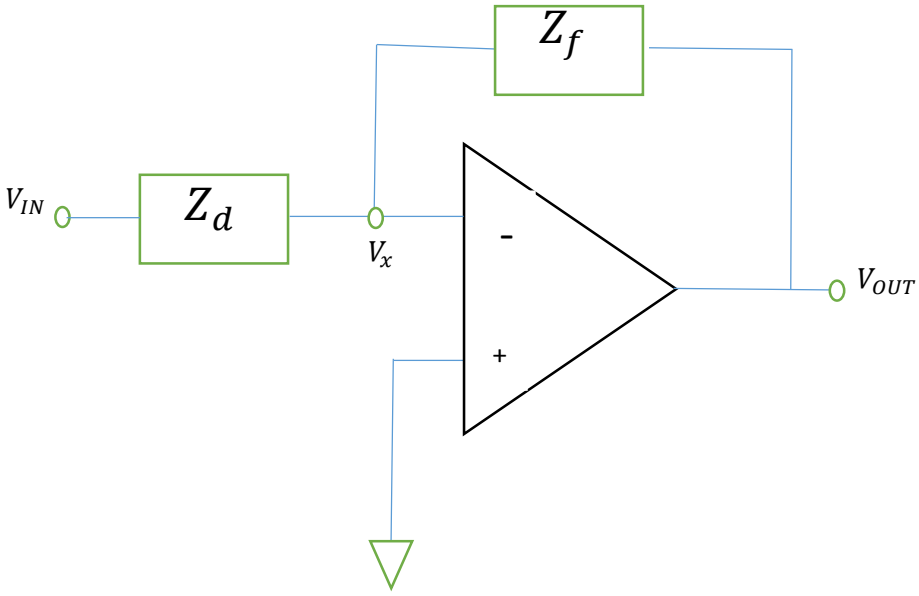

Figure 16: Circuit Schematic for op amp Bandwidth effects

We define the op amp to have a frequency-dependent gain that is given as $A(j\omega)$, which has both a magnitude and phase that are frequency dependent. We can then obtain a more accurate equation that relates the input voltage V_{IN} to the output voltage V_{OUT} for any feedback circuit. The derivation is shown below:

$$V_{OUT}(j\omega) = -V_X(j\omega)A(j\omega)$$

And then:

$$V_X(j\omega) = \frac{Z_f}{Z_f + Z_d}_X V_{IN}(j\omega) + \frac{Z_d}{Z_f + Z_d} V_{OUT}(j\omega)$$

Eliminating $V_X(j\omega)$ and solving for $\frac{V_{OUT}}{V_{IN}}(j\omega)$ we obtain:

$$\frac{V_{OUT}}{V_{IN}}(j\omega) = \frac{A(j\omega)}{1 + \frac{Z_f}{Z_d} + A(j\omega)} \frac{-Z_f}{Z_d}$$

From the above equation we see that as expected, the op amp gain function has an effect on the net transfer function for the impedance measurement system.

Let analyze a typical example for an impedance measurement setup for a biosensor for frequency range less than 30 KHz and a typical two-pole op amp. Putting the op amp gain in the form of magnitude-phase product, then the input-output equation can be re-written as:

$$\frac{V_{OUT}}{V_{IN}}(j\omega) = \frac{A(\omega)e^{j\phi(\omega)}}{1 + \frac{Z_f}{Z_d} + A(\omega)e^{j\phi(\omega)}} \frac{-Z_f}{Z_d}$$

Now suppose that:

I. The op amp has a Gain-Bandwidth product (GBP)of 3MHz, as in the internal op amps of the MAX32600
II. The system is operating at a frequency f_m of 12.5 KHz, a typical frequency over which the impedance of an electrical biosensor can be measured
III. Z_d is in the range 1nF-10nF Capacitor, which represents the typical impedance of a biosensor
IV. Z_f is 500pF Capacitor, which represents a typical value for the feedback capacitor in a biosensor application

Since the system is operating at 12.5 KHz then we can obtain approximate values for the magnitude and phase of the op amp as:

$A(\omega)|_{\omega=2\pi*12.5*10^3} = \frac{GBP}{f_m} = \frac{3*10^6}{12.5*10^3} = 240$ and

$\phi(\omega)|_{\omega=2\pi*12.5*10^3} \approx \pi/2$ since the frequency of 12.5 KHz is much larger than the first pole in the system and more than a decade below the second pole of a two-pole op amp Amplifier. Therefore we obtain that $A(j\omega)|_{\omega=2\pi*12.5*10^3} \approx 240j$.

Making the complete substitution for all the variables in the input-output equation we have that:

$$\frac{V_{OUT}}{V_{IN}}(j\omega)|_{\omega=2\pi*12.5*10^3} = \frac{240j}{1 + \frac{Z_f}{Z_d} + 240j} \frac{-Z_f}{Z_d}$$

Substituting in $Z_f = \frac{1}{C_f j\omega}$ and $Z_d = \frac{1}{C_d j\omega}$ then $\frac{Z_f}{Z_d} = \frac{C_d}{C_f}$ and then for:

a. $C_d = 1nF$ $\qquad \frac{V_{OUT}}{V_{IN}}(j\omega)|_{\omega=2\pi*12.5*10^3} = \frac{240j}{1+2+240j} * (-2)$

Knowing that the ideal gain would be (-2) a magnitude and phase error that results from the non-idealities of the op amp can be determined. Let G_{Mr} represent the magnitude and $G_{\phi r}$ represent the phase of the actual impedance measurement set up. Also let G_M represent the magnitude and G_ϕ represent the phase of the ideal impedance measurement set up (that would use an ideal op amp). Then we have that:

$$\frac{G_{Mr}}{G_M} = \frac{240}{\sqrt{(1+2)^2 + 240^2}} = 0.99992188$$

This results in an approximately 0.008% error in the impedance measurement of the magnitude for a 1nF Capacitor.

To get the phase error we calculate the difference between the phase measurement for the ideal and actual impedance measurement setups. We know that

$$G_{\phi r} - G_{\phi} = \frac{\pi}{2} - \arctan\left(\frac{240}{2+1}\right) = 0.01249Rad = 0.716^o$$

Therefore measuring the phase of 1nF capacitor using this setup with the provided Z_f will result in a phase error of 0.716^o due to the non-idealities of the op amp.

The steps above can be repeated for 10nF and 40nF capacitors (which are other typical values of biosensor capacitances) to get both the magnitude and phase errors resulting from the op amp bandwidth. Next, amplifiers with different GBP are used and the results for the gain error and phase error are tabulated below.

Capacitance	GBP=3MHz		GBP=50MHz		GBP=100MHz	
	Gain Error (%)	Phase Error (degrees)	Gain Error (%)	Phase Error (degrees)	Gain Error (%)	Phase Error (degrees)
1nF	0.008	0.7162^o	0.000	0.043^o	0.000	0.021^o
10nF	0.381	5.000^o	0.001	0.301^o	0.000	0.150^o
40nF	5.251	18.650^o	0.020	1.160^o	0.005	0.580^o

Table 3: Table for the Gain and Phase errors for op amps with different GBP

From Table 3 it is clear that to have an accurate measurement for a large range of capacitive impedances a GBP product of greater than 50MHz is required to have a phase error less than 1^o . This is much higher than the 3MHz on the MAX32600 op amps and therefore for the measurement stage op amp this setup required an external op amp. The external op amp used is the LT1805 amplifier with a GBP of 85 MHz, which is below 100MHz but above 50 MHz, and which should therefore have a phase error less than 1^o.

2.2.5 Switch Resistance

Depending on the impedance to be measured, the switch resistance might affect the impedance measurement accuracy. This section describes the effect that the switch resistance might have on the impedance measurement and how to improve the accuracy of the impedance measurement setup.

First consider that for switch i the switch resistance is $R_{s,i}$ and the impedance connected to it is $Z_{d,i}$. Also assume that the calibration impedance Z_{cal} is connected to the source voltage by a switch with an on resistance of R_{cal}. Then from the derivations in this chapter and adding the switch resistance we know that:

$$Z_{d,i} + R_{s,i} = \left(\frac{Y_{CAL}(s)}{Y_{Z_i}(s)}\right)(Z_{cal} + R_{cal})$$

Then $Z_{d,i}$ can be determined as:

$$Z_{d,i} = \left(\frac{Y_{CAL}(s)}{Y_{Z_i}(s)}\right)(Z_{cal} + R_{cal}) - R_{s,i}$$

Therefore ignoring the effect of the switch resistance $R_{s,i}$ on the magnitude and phase measurement leads to a measurement error. The value of this measurement error is related to the impedance to be measured. Considering typical values for biosensor impedances we could use a calibration impedance of 22nF and suppose one DUT is a 10nF Capacitor. Also according to the Datasheet of the MAX32600, the switch resistance is typically around 30 Ω so setting the typical value for $R_{s,i}$ =30 Ω. We can calculate the typical error in measuring a 10nF Capacitor. Ignoring the effect the switch resistance will have on the measurement will mean that the measured impedance is $Z_{d,i} + R_{s,i}$ but then we only expect it to be $Z_{d,i}$. Ignoring the the effect from R_{cal} we can determine that the magnitude error and phase error in measuring $Z_{d,i}$

$$MAG_{error} = \left(1 - \frac{\frac{1}{C_{d,i}\omega}}{\sqrt{{R_{s,i}}^2 + \frac{1}{C_{d,i}\omega}^2}}\right) * 100\%$$

$$PHASE_{error} = \frac{\pi}{2} - \arctan\left(\frac{1}{R_{s,i}C_{d,i}\omega}\right) = \arctan\left(R_{s,i}C_{d,i}\omega\right)$$

Substituting in the typical values for all variables such as $C_{d,i} = 10nF$, $\omega = 2\pi f_m = 2\pi * 12.5KHz$ and $R_{s,i} = 30\Omega$. Then

$$MAG_{error} = \left(1 - \frac{\frac{1}{(10 * 10^{-9})(2\pi * 12.5 * 10^3)}}{\sqrt{30^2 + \frac{1}{(10 * 10^{-9})(2\pi * 12.5 * 10^3)}^2}}\right) * 100\% = 0.028\%$$

$$\begin{aligned} PHASE_{error} = \arctan\left(R_{s,i}C_{d,i}\omega\right) &= \arctan(30 * (10 * 10^{-9})\,(2\pi * 12.5 * 10^3)) \\ &= 0.0235Rad \\ &= 1.35^o \end{aligned}$$

Ignoring the effect of the series resistance can have an effect on the accuracy of the impedance measurement (for example applications that might require a phase error less than 1^o). To reduce this effect on the accuracy of the measurement there is a need to calibrate out the switch resistances.

To calibrate out the switch resistance a switch calibration step is used. This step is carried out before an initial measurement is made. This step can be done with capacitors as the DUTs. Suppose the calibration capacitance is a known $C_{Cal} = 1nF$, then if we use a known DUT capacitor that is about 2 orders of magnitude larger than this capacitance and whose impedance plot is known, we can determine the

resistance of the switch in series with it. Because the DUT capacitance is 2 orders of magnitude larger than the calibration impedance then we can assume that the phase error is contributed entirely by the series resistance of the DUT capacitor. The phase error can be measured using the impedance measuring setup described previously above by averaging the phase in several frequency sweeps after which the switch resistance is determined as shown below.

$$\arctan\left(R_{s,i}C_{d,i}\omega\right) = PHASE_{error}$$

$$R_{s,i} = \frac{\tan(PHASE_{error})}{C_{d,i}\omega}$$

This measurement can be carried out over a frequency sweep and the approximate switch resistance can be determined as the averaged value for the determined resistances. The capacitances were measured using an impedance analyzer. The impedance analyzer used is the Agilent 4294A with an accuracy of about 0.08% (from the Agilent impedance analyzer manual) for impedance measurements in this range. This step can be repeated for all the other switches as well to determine all the switch resistances and calibrate them. Knowing the switch resistances, we can calibrate them out in the measurement. The calibration system we used calibrated the switch resistance once at the beginning of using the setup. A disadvantage with this setup would be that the switch resistance could change with time and even operating conditions such as temperature of the setup. For systems that require more measurement accuracy, recalibrating the switch resistances for every time a DUT is going to be determined can improve the accuracy. The improvement in accuracy due to this recalibrating will usually be a small one especially due to the estimates used to determine the value of the switch resistance.

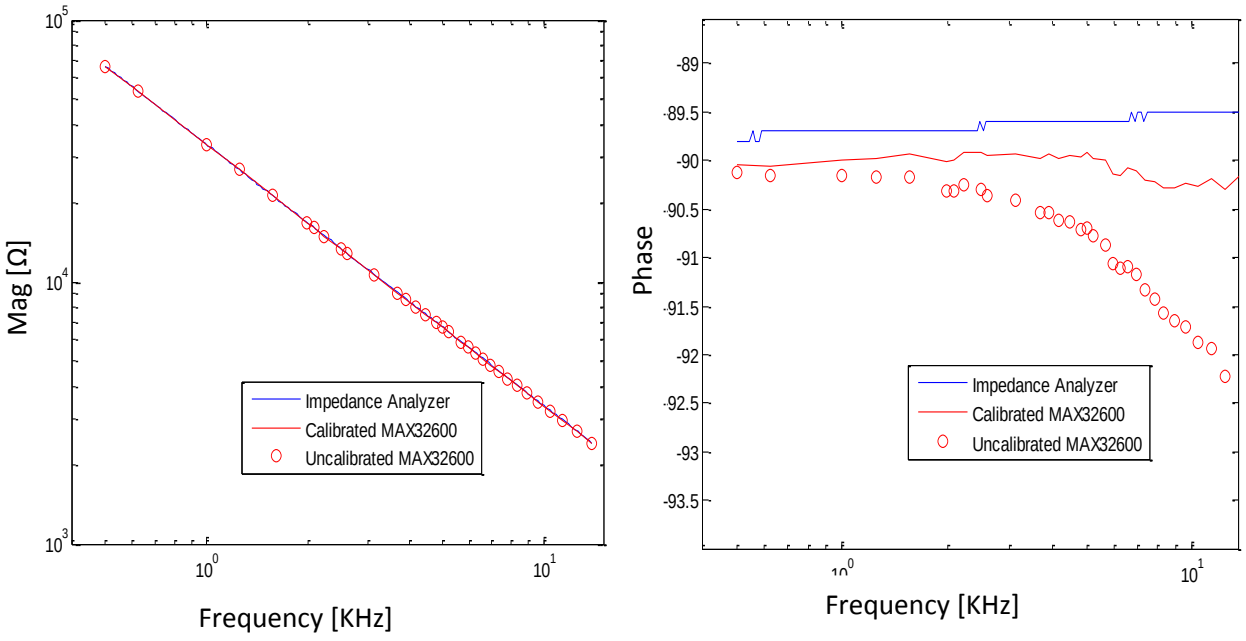

Figure 17: Plots showing the effect of switch resistance on Magnitude and Phase measurements

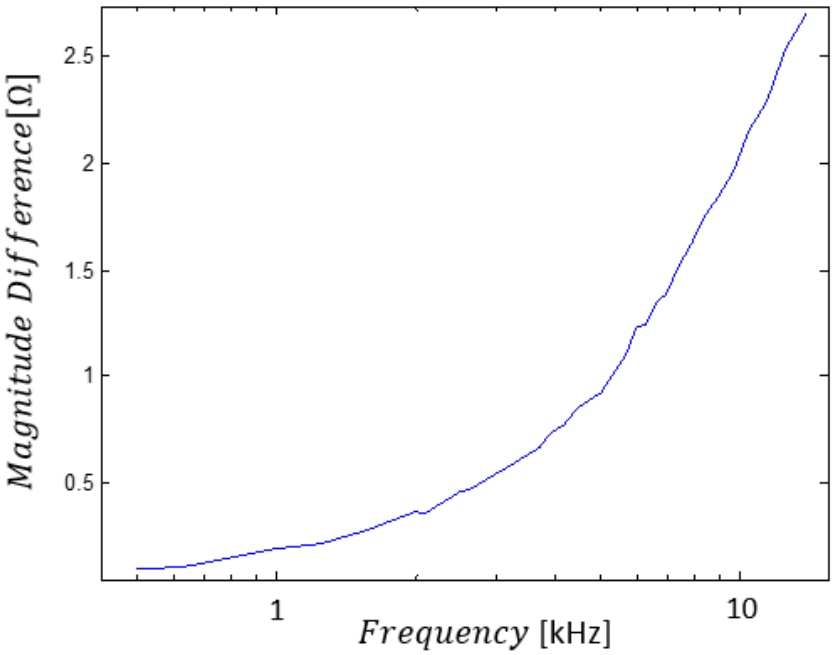

Figure 18: Plot for the Magnitude difference between the uncalibrated and calibrated MAX32600 setup

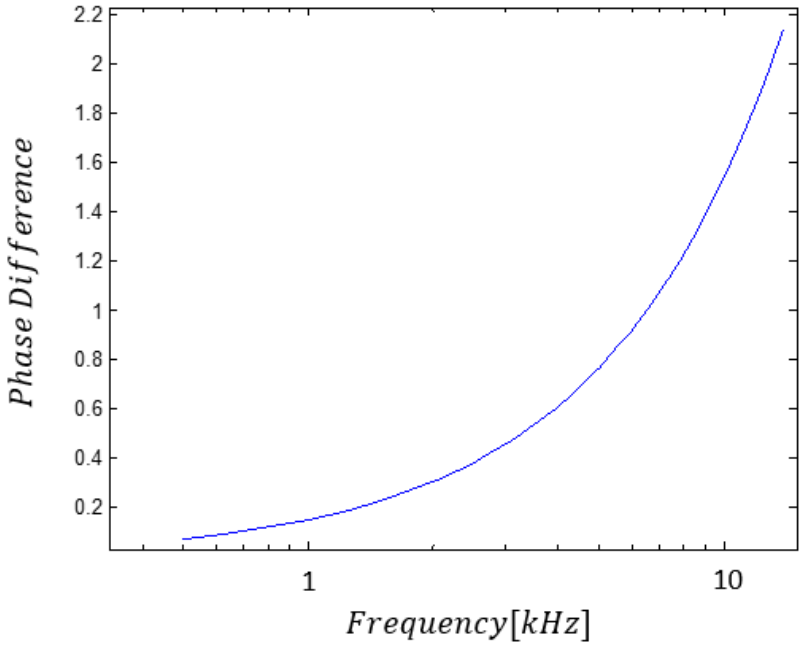

Figure 19: Plot for the phase difference between the uncalibrated and the calibrated MAX32600 setup

The Figure 17 above shows the effect of calibrating out the switch resistance on the magnitude and the phase while measuring a 4.7nF Capacitor. From Figure 17 the magnitude plot from the impedance analyzer is similar to that of both the calibrated and uncalibrated MAX32600 board measurement. The uncalibrated magnitude plot is close to the calibrated MAX32600 board measurement. This is shown by

the red plot showing calibrated MAX32600 measurement superimposing over the blue curve for the impedance analyzer. The two plots are close because the series switch resistance is small and has a small effect on the net magnitude, and thus calibrating it out has a negligible effect on the magnitude plot. On the other hand, the phase plot has a clear difference in the calibrated and uncalibrated phase. In fact calibrating out the switch resistance has an effect in improving the accuracy of the measured phase. For example for the 4.7nF capacitor measurement, adjusting for switch resistance reduces the phase difference with that of the Impedance Analyzer from 2.72^o to 0.64^o at 13.89 KHz. This is shown more clearly in the Figure 18 and Figure 19 where we only see a magnitude difference of 3Ω maximum but a phase difference of about 2.1^o between the calibrated (for switch resistance) and uncalibrated setups. Also note from the phase plot of the uncalibrated MAX32600 Board, that the phase error between the uncalibrated and the calibrated system is small for lower frequencies and increases with frequency as expected from the phase error equation.

2.3 Impedance meter trade-offs

We have shown several of the sources of measurement error in the designing an impedance analyzer. The three sources of error discussed are the op amp bandwidth, switch resistance and electronic noise especially in the measurement amplifier. Of these, with proper choice of the measurement amplifier, we can combat the op amp noise and effects that result from low op amp bandwidth with proper choice of the measurement op amp. The switch resistance has an effect on the phase measurement and without proper calibration might dominate the measured impedance error affecting the accuracy. Other factors that will affect the accuracy of the impedance meter would be accuracy in determining the calibration impedance magnitude and phase, measurement error from the ADC and drift in impedance value with temperature changes. The effects of these factors are not discussed because the first three factors dominate the error in the measured impedance value.

2.4 Conclusions

A complete impedance measurement setup was built based on the MAX32600 and several sources of measurement error are considered and steps to overcome these errors are considered. From the GBP product of the op amp to the switch resistance of the SPST to the input noise of the op amp used we consider how each of these factors affect the measurement accuracy. Steps are taken to combat these effect such when to calibrate out the switch resistance or to average several samples to overcome the noise in the circuit. Higher GBP op amps are also recommended to remove the magnitude and phase error in measured results.

After the complete system is built and analyzed we now apply to a real impedimetric biosensor. These results will be demonstrated in chapter 3.

Chapter 3: Impedance and biosensor measurement results

In this section we will describe actual impedance measurements using the setup described in the prior chapter. After careful choice of all the variables in the impedance measurement system such as Z_{CAL}, Z_f, the measurement op amp (bandwidth and noise characteristics should be acceptable) then we can test how accurate the system is. First several tests are carried out on actual known impedances measured using the impedance analyzer to determine how accurate the designed board compares to the Impedance analyzer. These plots are in the form of magnitude vs frequency and phase vs frequency plots for the required frequency range of the biosensor (500 Hz- 14 KHz). Next an actual biosensor is measured with a time-varying measurement showing the various changes in impedance with addition of different reagents and how this system can be used to sense a specific biomolecule.

3.1 Capacitor Measurements

In this section we will show capacitor measurements using the optimally chosen variables for the system.

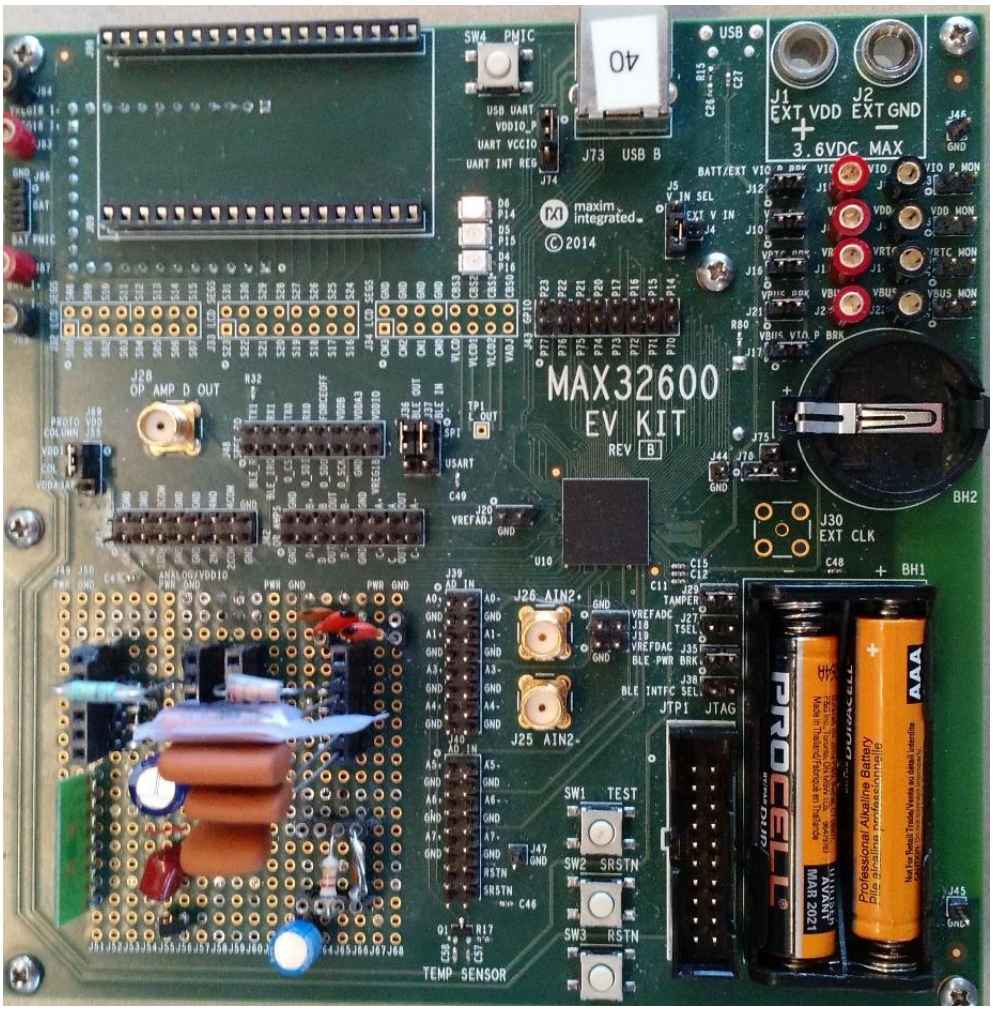

Figure 20: Picture showing the setup of the MAX32600 to measure 3 Capacitors

Figure 20 above shows the MAX32600 EvKit. The system, which was described in the previous chapter, uses batteries as power supply. The serial port on the EvKit is to interface with computer for post signal processing.

Measurement variables are optimally chosen to measure capacitive impedances in the range of 1nF-60nF. The choice of the feedback impedance is determined as a $C_f = 4.7nF$ in parallel with $R_f = 62\ k\,\Omega$. The calibration impedance is a capacitor $C_{cal} = 22nF$. Three capacitors are used, $C_1 = 4.7nF, C_2 = 10nF, C_3 = 32nF$ as the DUTs. The setup is similar to that in Section 2.2.2 **Choice of ZCAL**. An AC signal of magnitude 10mV$_{pp}$ is used as the input wave. A frequency sweep for the AC source from 500 Hz – 14 kHz is done. For each frequency point, the system measures the output voltage 400 times and does an averaging of these samples. The calibration impedance is also determined using an Agilent impedance analyzer using a frequency sweep in the same frequency range but with more frequency points (about 100) in a logarithmic spacing. For the measurement with the analyzer the AC drive wave is also 10 mV$_{pp}$. If a capacitor is used in the calibration path we can use the bode plot linearization to determine the calibration capacitance. The measured impedance is then determined using the MAX32600 and this measurement is compared with that obtained using an impedance analyzer. Each frequency measurement takes just over 1s with the whole frequency sweep taking 43.75s. In subsequent sweeps we were able to reduce the time for a complete sweep to about 10s.

Both the magnitude and phase are plotted versus frequency shown in the plot below.

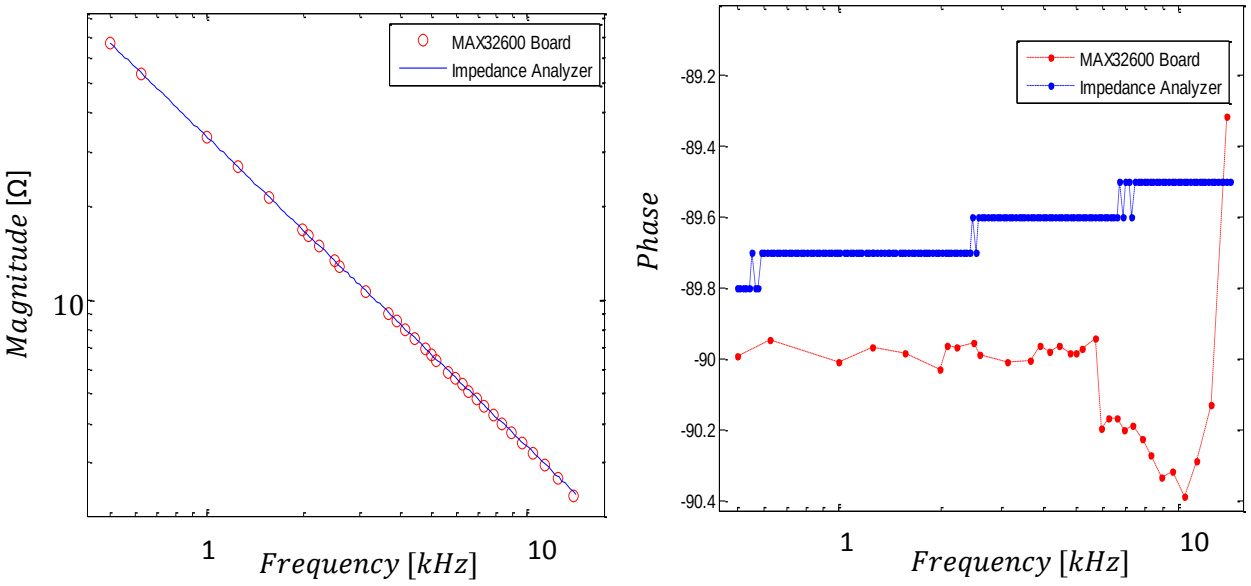

Figure 21: Magnitude and Phase plots of the Impedance Analyzer and the MAX32600 System for 4.7nF Capacitor

From Figure 21 the magnitude plot is close to the one obtained from the impedance analyzer and we can infer that the MAX32600 measurement setup is accurate enough to be used in a biosensor application. Comparing the magnitude plot from the impedance analyzer with that of the MAX32600 board, the percentage difference per frequency measurement can be. It was observed that this percentage difference increased with frequency and was higher at the higher frequencies. The maximum magnitude difference was 1.25% at 12.5 kHz. In estimating the accuracy of a capacitor the

system is accurate to 1% of the value determined from an Agilent Impedance analyzer. This is good enough for biosensor measurements since accuracy combined with precision are both important. The phase measurement on the other hand has a measurement difference with the Agilent Impedance analyzer ranging from 0.2^o to 0.9^o. The precision of the system can be determined by making a time varying measurement and obtaining the mean and variance of the measurement. To determine the precision of the system, a continuous time capacitive measurement is made for the above capacitors for 222 minutes. This is the equivalent to 302 continuous impedance measurements with each impedance measurement taking about 43.75s. To obtain the capacitance values we use curve fitting techniques on the magnitude and phase plots and estimate a capacitor value. These curve fitting techniques are described further in the next section.

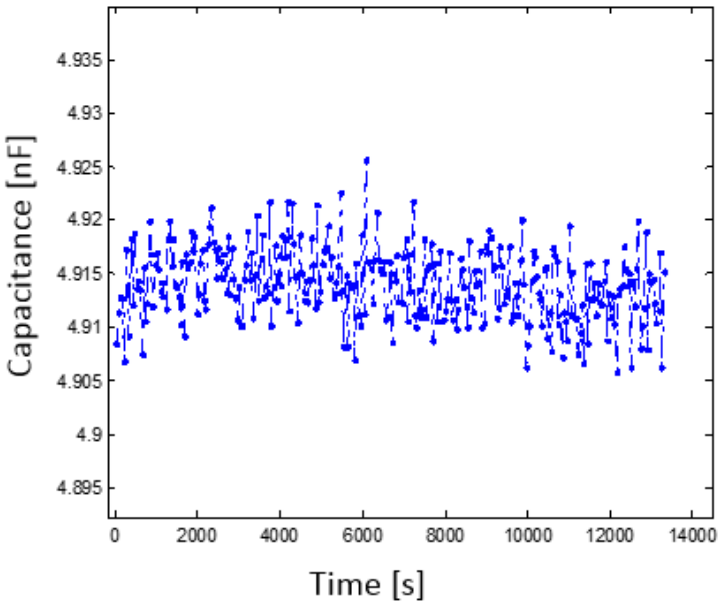

Figure 22: Measured capacitance over time for a 4.7nF Capacitor

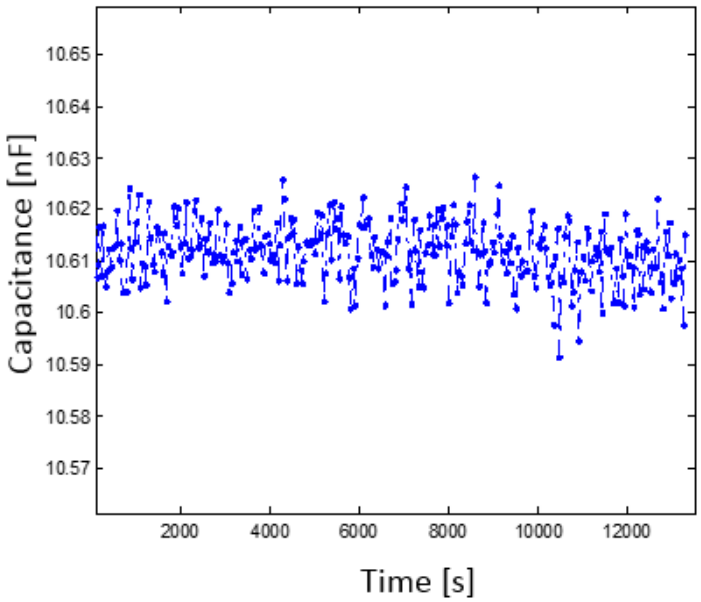

Figure 23: Measured capacitance over time for a 10nF Capacitor

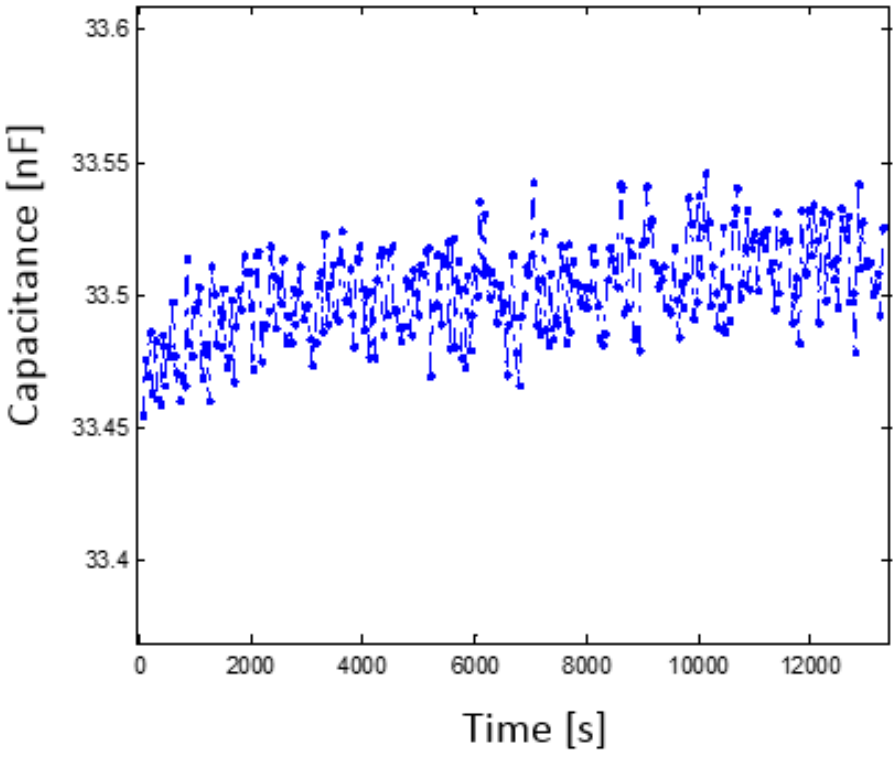

Figure 24: Measured capacitance over time for a 32nF Capacitor

Capacitance	Fractional RMS Variation[%]	Fractional peak to peak Variation [%]

4.7nF	0.0694	0.40
10nF	0.0541	0.33
32nF	0.0543	0.27

Table 4: Measurement Precision of the MAX32600 for 3 Capacitors

From Table 4 using the fractional RMS Variation that is determined as $\frac{\sigma_c}{\mu_c}$ where σ_c is the standard deviation in the measured capacitance and μ_c is the mean of the measured capacitance over time. This parameter is presented as the fractional RMS variation as a percentage. The maximum fractional variation is 0.07% for the 4.7nF Capacitor. This means that the system can measure with a certain precision a capacitance change of 0.07%*4.7nF which is 3.29pF capacitor change. Another parameter that can be used to determine precision is the fractional peak to peak variation in the measured capacitance. We see that the peak to peak variation in the measured impedance is below 0.4%. The peak fractional variation can then be estimated as about ½ of the result obtained for peak to peak variation.

3.2 MATLAB GUI

To display the measured results from the MAX32600 board we designed a MATLAB GUI for this purpose. The GUI collects the data from the MAX32600 board and does the post analysis plotting the time varying magnitude and phase plots and then estimation of the capacitance.

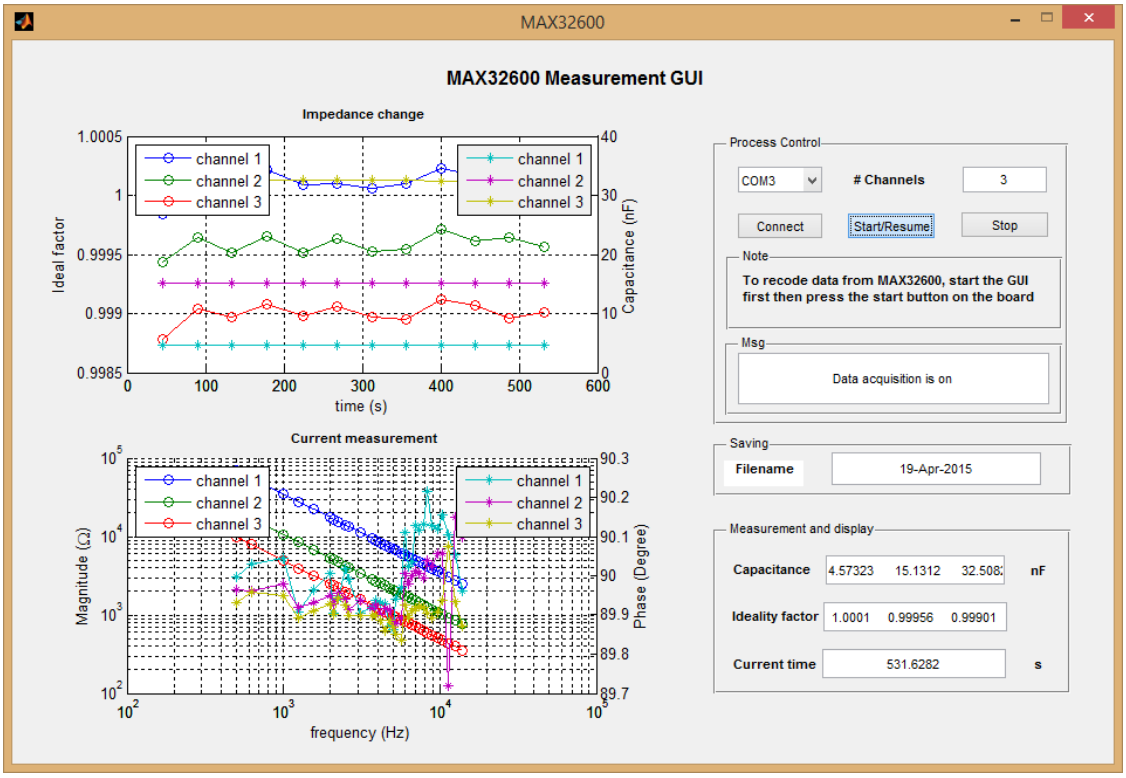

Figure 25: MATLAB GUI Layout

Shown in Figure 25 is the Matlab GUI layout. The GUI is setup with 3 main sections described below.

I. The Process control section.

This is used to acquire data from the MAX32600. The Connect button is used to make a connection with the MAX32600 board using a serial cable at a given Baud rate. This button means we are ready to receive data from the MAX32600 board. The next button is the start button which means to start acquiring the data that is coming out from the MAX32600 board. The data received at this point contains the magnitude and phase values. Pressing the start button again will finish a frequency sweep and then pause the process of obtaining results from the MAX32600. The last button is the stop button which ends a measurement when the current frequency sweep is done.

II. Measurement and display section
This section displays three important results. The measured capacitance for each device, the ideality factor and finally the measurement time. Part of this section will describe the complete process for determining the measured capacitance.

III. Plotted results.
The results are then plotted on two graphs. One the graphs shows the time varying capacitance and ideality factor and the other is for the bode plots showing how the magnitude and phase vary for each frequency sweep. The second plot (bode plot) gets replaced by a new one every time a frequency sweep is done. At the end of the process, all important variables are saved as Matlab file in the format shown in the GUI (if the file name is not changed).

3.2.1: Determination of the capacitance values and biosensor modelling

Even after the magnitude and phase values are obtained from the MAX32600 board, the determination of the actual capacitance of a capacitor is not straightforward. Because the values obtained from the magnitude plot won't be exact, some form of curve fitting is required to determine an estimate of the actual capacitance. The Matlab function polyfit does the work of curve fitting since the bode plot for a capacitor is a linear plot in the log log domain. All these steps are shown in the Matlab GUI code in the appendix of this thesis.

Biosensors are imperfect capacitors that display a double layer property. This capacitive imperfection is modelled electrically as a constant phase element. The electric model is as below:

$$Z_d = \frac{1}{C_d(j\omega)^{\eta}}$$

Taking logarithms of the magnitude of both sides we get that:

$$\log(Z_d) = -\log(C_d) - \eta\log(\omega)$$

Which is in the form of $y = c - \eta x$ where y is the $\log(Z_d)$, $x = \log(\omega)$ and $c = -\log(C_d)$, where C_d is the capacitive property of the biosensor and η is the exponent of the constant phase element. For an ideal capacitor $\eta = 1$ as expected. After obtaining values for the magnitude and the phase from the MAX32600 board, we can determine several of the variables. η can be estimated as the average phase value over the measurement frequency range. Another way to estimate η is using the slope of the curve fitted magnitude plot in log-log axes. For our system we used the phase averaging because it provided better precision (less capacitance drift with time) for the determined capacitance. After the value of η is

estimated, using curve fitted parameters, we can obtain an estimate for the capacitance of the biosensor C_d. The steps are described mathematically below:

$$\mathrm{p} = \mathrm{polyfit}(\mathrm{x}, \mathrm{y}, 1)$$

$$\mathrm{q} = \mathrm{p}(2) \text{ and } \mathrm{p} = \mathrm{p}(1)$$

p representing the slope and q representing the y-intercept. Then we can determine that

$$\mathrm{c} = \mathrm{q}$$

Knowing c we can determine the unknown capacitance C_d as

$$C_d = \exp(-\mathrm{c})$$

This process is repeated over time to obtain the time varying measurement of the biosensor capacitor.

3.3 Capacitor change measurement

The section explores the accuracy and precision of measurement of the MAX32600 board setup when measuring capacitor changes. Because biosensors should be optimized to measure changes in properties (such as capacitance in our case) and not the absolute values of these properties, then to test the MAX32600 setup to do the readout process we will use actual capacitors and measure changes in the capacitor values.

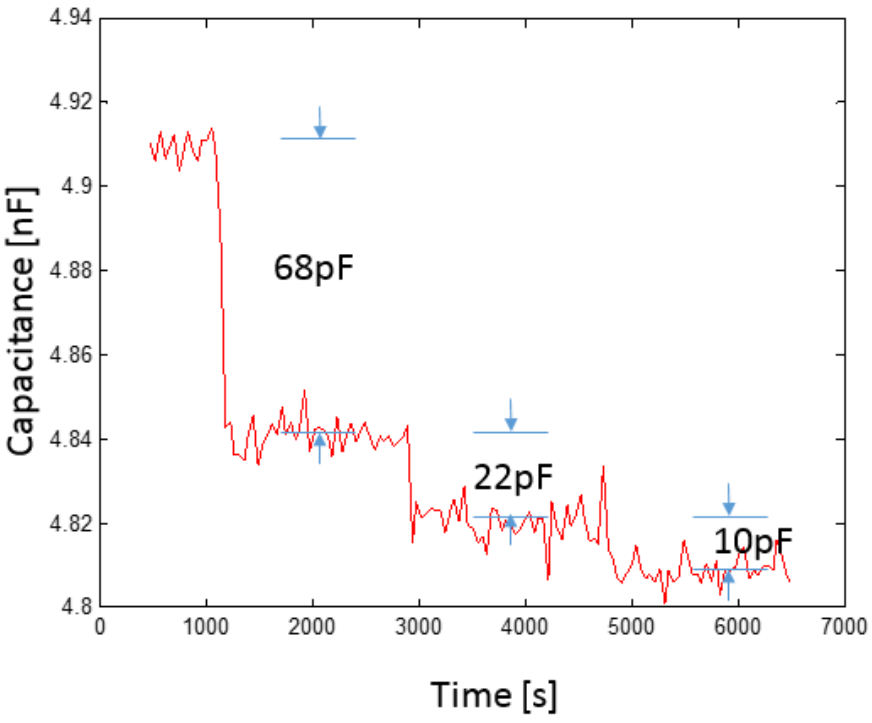

Figure 26: Capacitor change measurement for a 4.91nF Capacitor

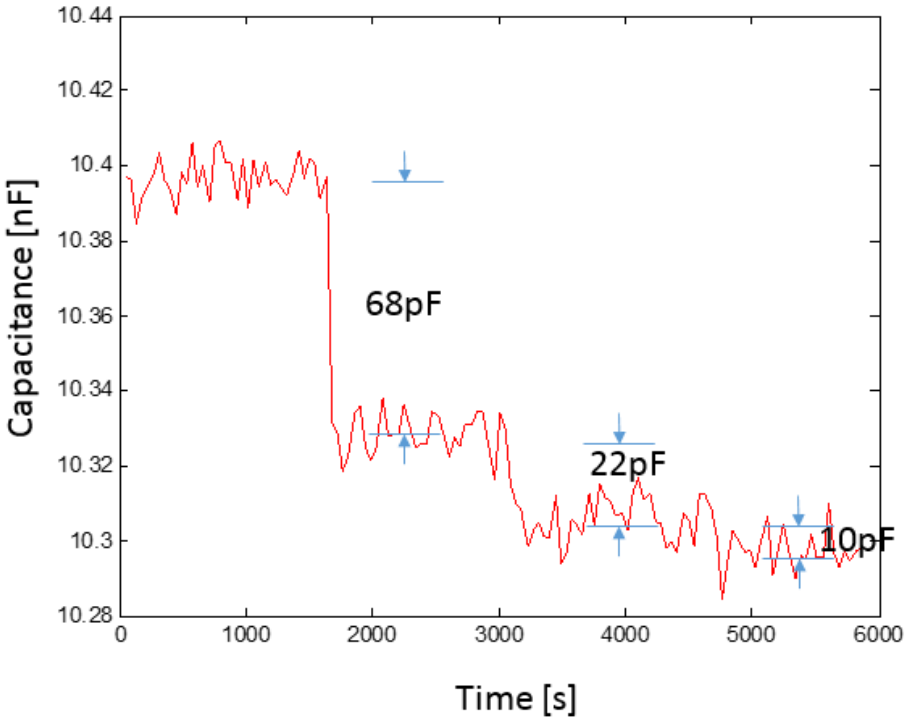

Figure 27: Capacitor change measurement for a 10.397nF Capacitor

In order to test how accurately the system can measure changes in capacitance we used a constant capacitor with capacitance either 4.9nF or 10.397nF and in parallel with it we had one 68pF capacitor, one 22pF Capacitor and another 10pF capacitor. First we removed the 68pF from the combination and measured the resulting capacitance, then removed the 22pF and finally the 10pF. The system was still able to determine the change in capacitance for a 10pF capacitor for both a 4.9nF capacitor and a 10.397nF setup. The change for a 4.9nF capacitor is in fact easier to determine than with that of a 10.397nF capacitor. For each of these systems the measurement precision can be determined as

$Precision = \frac{\Delta C}{C} * 100\% = \frac{10pF}{10.397nF} * 100\% = 0.096\%$ for the system with a 10nF capacitor.

Next estimating the accuracy for each change in capacitance we determine the accuracy in estimating the small changes in capacitance above. This change was determined as

$$\frac{\Delta C\_measured}{\Delta C\_actual}.$$

The results are obtained as 1.5% for 68pF capacitance change, 3.6% for 22pF capacitance change, and 5.1% for 10pF capacitance change for a 10nF capacitor measurement system. As expected the measurement accuracy is reduced as we measure smaller changes in capacitance.

3.4 Measuring a Biosensor Impedance

Next we use the MAX32600 board to measure the impedance of an actual biosensor and the plot the capacitance variation with time. This section will describe the process of making an impedimetric biosensor and a lab measurement using the biosensor.

The impedimetric biosensor is composed of interdigitated gold electrodes (IDE). These electrodes are the basis for the formation of a capacitor of the sensor. The separation of the electrodes is usually on the order of a few microns for capacitors in the range of several nanoFarads. The sensor is then built using a SAM that separates the gold electrodes from the antibody molecules. To immobilize the antibody onto the IDE, SA is added that specifically binds to a biotin molecule. This will allow for only specific binding of the antibody and the associated antigen to be detected. The channel lets in the several buffers used to build the biosensor and also the sample under test. Below we discuss further using this channel and the procedures taken to test, prepare and calibrate the impedimetric biosensor.

3.4.1: Pre-measurement sensor test

The sensor at this step is a channel of IDEs with SAM molecules on it. This step is used to check whether the sensor meets specification to be used as a biosensor. In this step we remove the effect of non-specifically bound molecules and gauge the impedance range of the sensor. The steps in the process are graphically shown and described below:

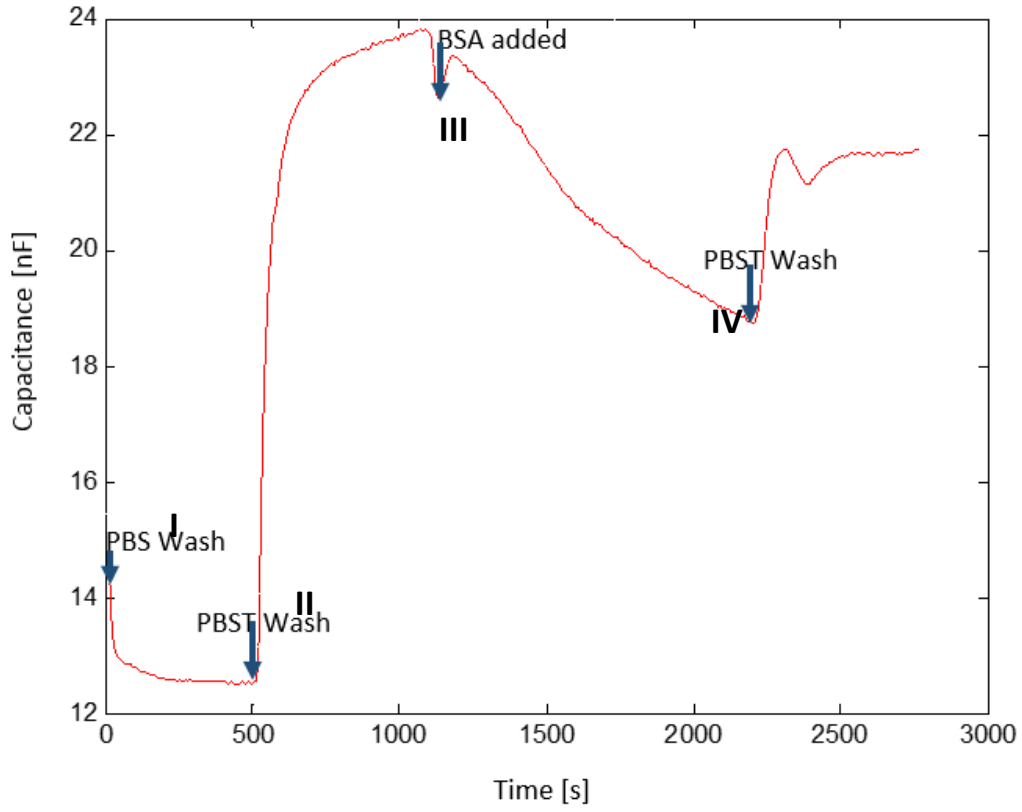

Figure 28: Plot showing steps in the pre-measurement sensor checkout step

I. Add PBS (Phosphate Buffered Saline) buffer for 10 minutes. During this step, the capacitance of the biosensor will normally decrease. There is a drift in the capacitance of the biosensor.
II. Add PBST buffer for 10 minutes. PBST is the same as PBS with an organic detergent that is known as Tween (T). After this step the capacitance increases usually 10-20%.
III. Add bovine serum albumin (BSA) for 20 minutes. The BSA was added to remove the effect of non-specific binding in the biosensor. After this step the capacitance will decrease as shown in Figure 28.
IV. Add PBST buffer for 10 minutes. The capacitance increases.

When the pre-measurement sensor test procedure is done, building the complete sensor can then be started.

3.4.2: Building the sensor

After making sure the sensor is acceptable, then next step is to complete the building process of the sensor. This step involves adding SA to which the antibody gets to bind. The steps in this process are graphically shown and then described below:

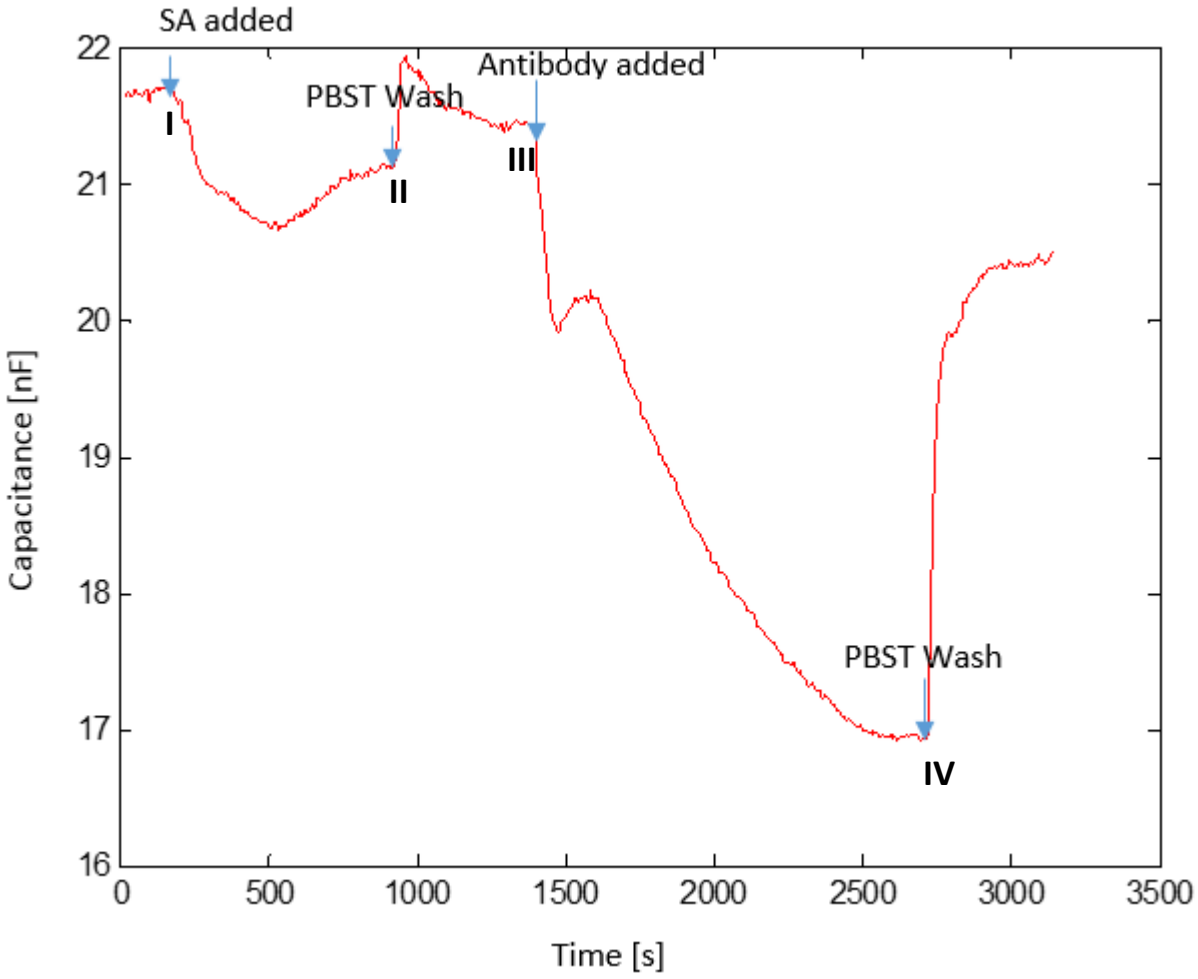

Figure 29: Plot showing steps in building the sensor step

I. Add 40µg/ml of SA for 15 minutes. The SA, which binds with the SAM, allows for the binding of the antibody.
II. Add PBST buffer for 10 minutes. PBST will wash away the SA molecules that are not bound on the SAM
III. Add 80µg/ml of antibody for 20 minutes. The antibody will then get bound to the SA molecules that are already bound on the SAM.
IV. Wash with PBS for 10 minutes.

3.4.3: Actual sensor measurement

When the complete sensor is built then actual measurements are carried out on the sensor. The steps are shown graphically and described below.

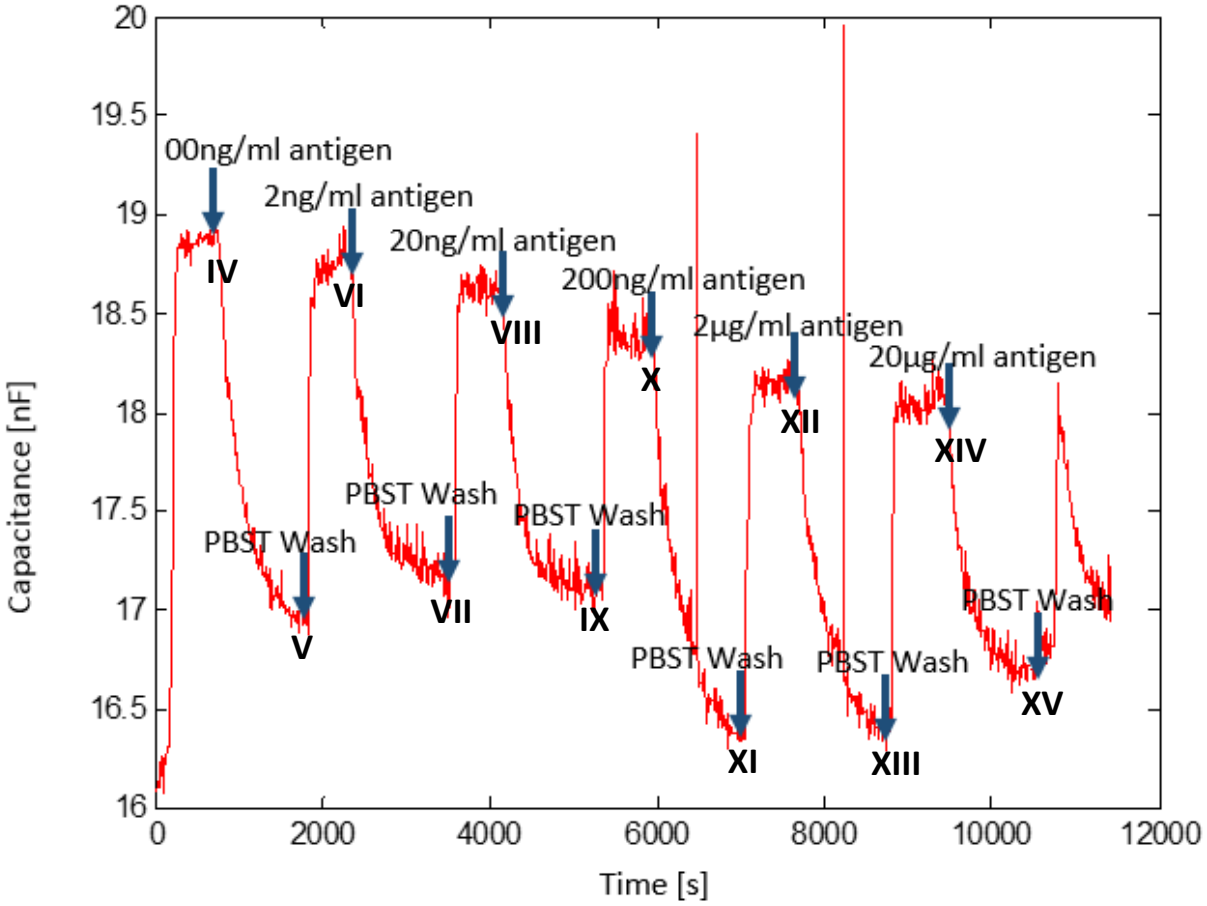

Figure 30: Plot showing steps in actual sensor measurement step

I. Add BSA for 10 minutes. This step is to test for non-specific binding of molecules. After this step the capacitance decreases.
II. Wash with PBS for 10 minutes (Did this for 15 minutes). The capacitance didn't decrease at this step.
III. Wash with PBST for 10 minutes. The capacitance increases, in fact it is supposed to increase back to the initial value before BSA was added.
IV. Add the antigen at 00ng/ml for 20 minutes. The capacitance decreases but this is due non-specifically bound molecules since there is no antigen in the buffer.
V. Wash with PBST for 10 minutes. The capacitance is supposed to return to its initial value.
VI. Add the antigen at 2ng/ml for 20 minutes. The capacitance should decrease again.
VII. Wash with PBST for 10 minutes. This again will remove the non-specifically bound molecules from the previous interaction.
VIII. Add the antigen at 20ng/ml for 20 minutes. The capacitance should decrease again.
IX. Wash with PBST for 10 minutes.
X. Add the antigen at 200ng/ml for 20 minutes. The capacitance should decrease again.

XI. Wash with PBST for 10 minutes.
XII. Add the antigen at 2µg/ml for 20 minutes. The capacitance should decrease again.
XIII. Wash with PBST for 10 minutes.
XIV. Add the antigen at 20µg/ml for 20 minutes. The capacitance should decrease again.
XV. Wash with PBST for 10 minutes.

The capacitor change at each step can be plotted against the concentration as shown below.

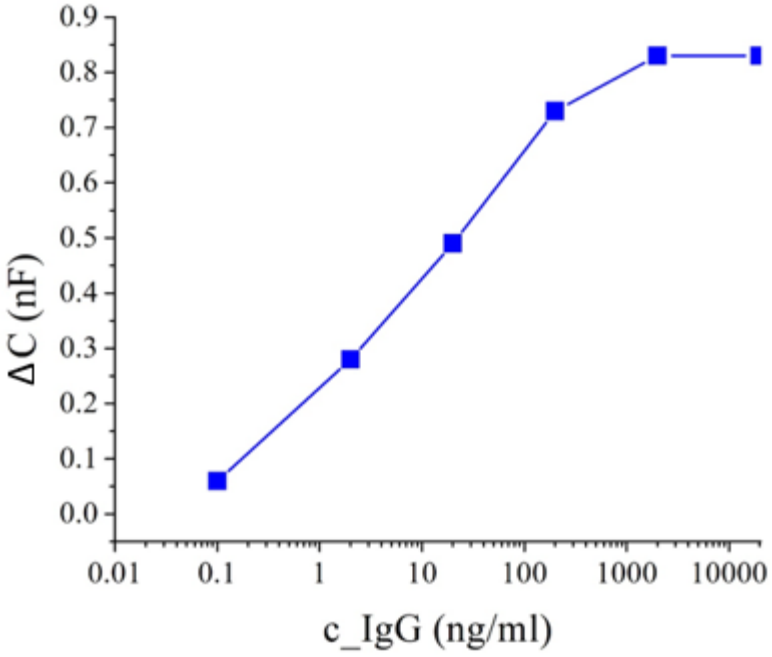

Figure 31: Capacitor change against antibody concentration

Figure 31 shows the change in capacitance measured by the impedance meter system for different antigen concentrations added. The impedance measurement system is able to detect small changes in capacitance as determined previously when ideal capacitors were measured. This experiment was repeated to determine the repeatability property of the biosensor but same results could not be attained. Therefore Figure 31 only demonstrates the ability of the impedance measurement setup to measure small capacitor changes rather than an achieved sensitivity of this particular biosensor.

Chapter 4: Conclusion and Future work

4.1 Summary and contributions

We have described a readout system for biosensor point of care testing systems. The system that is based on the MAX32600 Embedded system was 1% accurate with a precision of about 0.1%. The system was able to achieve the goal of a portable and relatively accurate impedance measurement setup for impedimetric biosensor applications. In this chapter we will describe the contributions of this work.

Impedance measurement systems that require multiplexing are affected in accuracy by the on resistance of the switches used. A lot of the available systems ignore the effect of the resistance of the switches on accuracy. In our system that used the MAX32600 with an SPST switch having on resistance around 30Ω we showed analytically how the switch resistance affects the accuracy of the measurement system and devised a calibration method to improve the measurement accuracy of the system. The system was able to make more accurate measurement with a phase measurement improvement of about 2^o for high frequency (~14 kHz) measurements.

Another contribution in this thesis is the analysis of the op amp bandwidth. Most impedance measurement systems that use the auto-balancing bridge method use high bandwidth op amps or transimpedance amplifiers to have a good accuracy. These systems usually do not analytically explain the need for the high bandwidth and the effects the op amp bandwidth has on the accuracy of the system. In Chapter 2 we described the effect of the op amp bandwidth on the measurement accuracy and selected an optimal bandwidth so the op amp's bandwidth had minimal effect on the accuracy of the measured impedance.

4.2 Future work

For future work, we describe below.

Ability to do a differential measurement. The system we designed has the potential to be used a differential sensor. The way the current sensor works is by measuring two sensors separately and then determining the difference of the impedance measured after readout. A better system for a differential sensor might be to electrically measure the differential signal and then determine the differential impedance of the sensors.

From chapter 2 we saw how the switch resistance affected the accuracy of the readout system when a multiplexed measurement is required. To improve the accuracy of the measurement we calibrated out the switch resistance. We saw the problem with this method was that it is difficult to accurately determine the switch resistance so we can calibrate it out. The switch resistance also varies with temperature and other conditions. Therefore to mitigate all these problems associated with switch resistance a better model might use low on-resistance switches for the applications that will require multiplexing and thus removing the need to calibrate out the switch resistance.

Also from chapter 2 we described the steps used to choose the calibration impedance. We noted that the calibration impedance was chosen depending on the precision requirement. The limit on the accuracy was determined to be 1%. A future step would involve examining the effect on the choice of the calibration impedance on the actual accuracy of the measurement of the DUTs.

The current readout system was accurate for measurements of impedance in the frequency range of 500 Hz – 14 kHz. This is a small range for some biosensor applications. In fact some biosensor applications do impedance measurement up to 100 kHz and even above that. An area of research would

be how to accurately measure impedance up to a frequency as high as 100 kHz while maintaining the accuracy for the frequency range of 500 Hz – 14 kHz.

Finally for the impedimetric biosensor after determining a board level application that can accurately determine impedances such as described above using the MAX32600 design of an integrated circuit that incorporates the sensor and the readout system would be an excellent goal. This integrated system would lead to a more accurate system by limiting all noise sources. Another advantage that the integrated system presents is a more miniaturized system making the system more portable and a better alternative for point of care testing.

Appendix

Matlab GUI Code:

```
function varargout = MAX32600(varargin)
% MAX32600 MATLAB code for MAX32600.fig
%      MAX32600, by itself, creates a new MAX32600 or raises the existing
%      singleton*.
%
%      H = MAX32600 returns the handle to a new MAX32600 or the handle to
%      the existing singleton*.
%
%      MAX32600('CALLBACK',hObject,eventData,handles,...) calls the local
%      function named CALLBACK in MAX32600.M with the given input arguments.
%
%      MAX32600('Property','Value',...) creates a new MAX32600 or raises the
%      existing singleton*.  Starting from the left, property value pairs are
%      applied to the GUI before MAX32600_OpeningFcn gets called.  An
%      unrecognized property name or invalid value makes property application
%      stop.  All inputs are passed to MAX32600_OpeningFcn via varargin.
%
%      *See GUI Options on GUIDE's Tools menu.  Choose "GUI allows only one
%      instance to run (singleton)".
%
% See also: GUIDE, GUIDATA, GUIHANDLES

% Edit the above text to modify the response to help MAX32600

% Last Modified by GUIDE v2.5 07-Oct-2014 10:25:56

% Begin initialization code - DO NOT EDIT
gui_Singleton = 1;
gui_State = struct('gui_Name',       mfilename, ...
    'gui_Singleton',  gui_Singleton, ...
    'gui_OpeningFcn', @MAX32600_OpeningFcn, ...
    'gui_OutputFcn',  @MAX32600_OutputFcn, ...
    'gui_LayoutFcn',  [] , ...
    'gui_Callback',   []);
if nargin && ischar(varargin{1})
    gui_State.gui_Callback = str2func(varargin{1});
end

if nargout
    [varargout{1:nargout}] = gui_mainfcn(gui_State, varargin{:});
else
    gui_mainfcn(gui_State, varargin{:});
end
% End initialization code - DO NOT EDIT


% --- Executes just before MAX32600 is made visible.
function MAX32600_OpeningFcn(hObject, eventdata, handles, varargin)
% This function has no output args, see OutputFcn.
% hObject    handle to figure
```

```
% eventdata  reserved - to be defined in a future version of MATLAB
% handles    structure with handles and user data (see GUIDATA)
% varargin   command line arguments to MAX32600 (see VARARGIN)

% Choose default command line output for MAX32600
handles.File_name =  date;
handles.beta = [];
handles.C = [];
handles.T = [];

handles.frequency=1.0e3*[0.5 0.625 1 1.25 1.5625 1.9841 2.0833 2.2321 2.5...
    2.6042 3.125 3.6765 3.9062 4.16667 4.4643 4.8077 5 5.2083 5.6818...
    5.9524 6.25 6.5789 6.94444 7.3529 7.8125 8.33333 8.9286 9.6154...
    10.4167 11.3636 12.5 13.8889];
handles.Channels_num =
str2double(get(findobj(hObject,'Tag','Channels'),'String'));
set(handles.Filename,'String', handles.File_name);
handles.output = hObject;
guidata(hObject, handles);

% --- Outputs from this function are returned to the command line.
function varargout = MAX32600_OutputFcn(hObject, eventdata, handles)
% varargout  cell array for returning output args (see VARARGOUT);
% hObject    handle to figure
% eventdata  reserved - to be defined in a future version of MATLAB
% handles    structure with handles and user data (see GUIDATA)

% Get default command line output from handles structure
varargout{1} = handles.output;

% --- Executes on button press in Connect.
function Connect_Callback(hObject, ~, handles)
% hObject    handle to Connect (see GCBO)
% eventdata  reserved - to be defined in a future version of MATLAB
% handles    structure with handles and user data (see GUIDATA)
try
    sport = serial(handles.COM);
    sport.Terminator = 'LF';
    sport.BaudRate = 115200;
    sport.DataBits = 8;
    sport.StopBits =1;
    sport.InputBufferSize = 50000;
    sport.Timeout = 2;
    fopen(sport);
    flushinput(sport);
    handles.fID = fopen([handles.File_name '.txt'],'w');
    msg = fgetl(sport);
    while isempty(msg)
        msg = fgetl(sport);
    end
    set(handles.Msg,'String',msg);
    handles.sport = sport;
    handles.output = hObject;
    guidata(hObject, handles);
catch err
    fclose(handles.fID)
```

```
    fclose(sport)
    err.message
    save err.mat err
end

% --- Executes on button press in Start.
function Start_Callback(hObject, eventdata, handles)
% hObject    handle to Start (see GCBO)
% eventdata  reserved - to be defined in a future version of MATLAB
% handles    structure with handles and user data (see GUIDATA)
beta = handles.beta;
C = handles.C;
T = handles.T;
sport = handles.sport;
N = length(handles.frequency);
M = handles.Channels_num;
data = zeros(N,M*2);
Rc = 26.351;% calibration resistance
R = [27.157 27.523 28.12];
Ccal=21.127e-9; % Calibration capactiance; Ccal1=[21.7964,15.00
frequency = handles.frequency;
omega = 2*pi*frequency;
Zcx =(Rc+(1./(Ccal.*omega*1i)));
%Zcx=10e3*ones(1,N)
try
    while get(hObject,'Value')
        tic
        set(handles.Msg,'String','Data acquisition is on');
        %% Retrieve data from UBS port
%         msg = fgetl(sport);
        N;
        for k = 1:N
            d = str2num(sprintf('%c',fgetl(sport)));
            while isempty(d)
                d = str2num(sprintf('%c',fgetl(sport)));
            end
            data(k,:) = d;
        end
        data(:,1:M) = (data(:,1:M).*(exp(1i.*data(:,1 +
M:end))).*repmat(Zcx(:),1,M))/1e4 ...
            - repmat(R(1:M),N,1);
        Mag = abs(data(:,1:M));
        Pha = - angle(data(:,1:M))/pi*180;

        %% Extract capacitance and ideality factor
        a = mean(Pha,1)/90;
        b = exp(mean(-log(Mag) - log(omega(:))*a,1));
        C = [C;b];
        beta = [beta;a];
        if isempty(T)
            t = toc;
        else
            t = T(end) + toc;
        end
        T = [T;t];
        %% Display the result
```

```
        set(handles.Ideality_factor,'String',num2str(a));
        set(handles.Capacitance,'String',num2str(b*1e9));
        set(handles.Current_time,'String',num2str(t));

        %% Plot the result
        axes(handles.Capacitance_ideality)
        [AX1,H1,H2] = plotyy(T,beta,T,C*1e9);
        set(get(AX1(1),'Ylabel'),'String','Ideal factor');
%         set(H1,'Marker','o');
        set(get(AX1(2),'Ylabel'),'String','Capacitance (nF)');
%         set(H2,'Marker','*');
        xlabel('time (s)');
        grid on
%         switch M
%             case 1
%                 legend(H1,'Location','NorthWest','channel 1');
%                 legend(H2,'Location','NorthEast','channel 1');
%             case 2
%                 legend(H1,'Location','NorthWest','channel 1','channel 2');
%                 legend(H2,'Location','NorthEast','channel 1','channel 2');
%             case 3
%                 legend(H1,'Location','NorthWest','channel 1','channel
2','channel 3');
%                 legend(H2,'Location','NorthEast','channel 1','channel
2','channel 3');
%         end
        axes(handles.Impedance_phase)
        [AX2,H3,H4] =
plotyy(frequency(:),Mag,frequency(:),Pha,@loglog,@semilogx);
        set(get(AX2(1),'Ylabel'),'String','Magnitude (\Omega)');
        set(H3,'Marker','o');
        set(get(AX2(2),'Ylabel'),'String','Phase (Degree)');
        set(H4,'Marker','*');
        xlabel('frequency (Hz)');
        grid on
        switch M
            case 1
                legend(H3,'Location','NorthWest','channel 1');
                legend(H4,'Location','NorthEast','channel 1');
            case 2
                legend(H3,'Location','NorthWest','channel 1','channel 2');
                legend(H4,'Location','NorthEast','channel 1','channel 2');
            case 3
                legend(H3,'Location','NorthWest','channel 1','channel
2','channel 3');
                legend(H4,'Location','NorthEast','channel 1','channel
2','channel 3');
        end
        pause(1)
        %% save data to .txt file
%         save(handles.File_name,'beta','C','T');
%         set(handles.Msg,'String','Data acquisition is paused!');
        switch M
            case 1
                fprintf(handles.fID,'%12.4f %12.4f\n',[Mag Pha]);
            case 2
```

```
                fprintf(handles.fID,'%12.4f %12.4f %12.4f %12.4f\n',[Mag
Pha]);
            case 3
                fprintf(handles.fID,'%12.4f %12.4f %12.4f %12.4f %12.4f
%12.4f\n',[Mag Pha]);
        end

    end
    save(handles.File_name,'beta','C','T');
    set(handles.Msg,'String','Data acquisition is paused!');
catch err
    save(handles.File_name,'beta','C','T');
    switch M
        case 1
            fprintf(handles.fID,'%12.4f %12.4f\n',[Mag Pha]);
        case 2
            fprintf(handles.fID,'%12.4f %12.4f %12.4f %12.4f\n',[Mag Pha]);
        case 3
            fprintf(handles.fID,'%12.4f %12.4f %12.4f %12.4f %12.4f
%12.4f\n',[Mag Pha]);
    end
    fclose(handles.sport)
    fclose(handles.fID)
    err.message
    set(handles.Msg,'String','Data acquisition is paused!');
end
% --- Executes on button press in Stop.
function Stop_Callback(hObject, eventdata, handles)
% hObject    handle to Stop (see GCBO)
% eventdata  reserved - to be defined in a future version of MATLAB
% handles    structure with handles and user data (see GUIDATA)
fclose(handles.sport);

fclose(handles.fID);
clear handles.sport;
set(handles.Msg,'String','Record stopped and serial port closed');
handles.output = hObject;
guidata(hObject, handles);

function Filename_Callback(hObject, eventdata, handles)
% hObject    handle to text12 (see GCBO)
% eventdata  reserved - to be defined in a future version of MATLAB
% handles    structure with handles and user data (see GUIDATA)
handles.File_name = get(findobj(hObject,'Tag','Filename'),'String');
guidata(hObject, handles);


function Filename_CreateFcn(hObject, eventdata, handles)
% hObject    handle to text12 (see GCBO)
% eventdata  reserved - to be defined in a future version of MATLAB
% handles    empty - handles not created until after all CreateFcns called

% Hint: edit controls usually have a white background on Windows.
%       See ISPC and COMPUTER.
if ispc && isequal(get(hObject,'BackgroundColor'),
get(0,'defaultUicontrolBackgroundColor'))
```

```
    set(hObject,'BackgroundColor','white');
end
% --- Executes during object creation, after setting all properties.
function text12_CreateFcn(hObject, eventdata, handles)
% hObject    handle to text12 (see GCBO)
% eventdata  reserved - to be defined in a future version of MATLAB
% handles    empty - handles not created until after all CreateFcns called

% Hint: edit controls usually have a white background on Windows.
%       See ISPC and COMPUTER.
if ispc && isequal(get(hObject,'BackgroundColor'),
get(0,'defaultUicontrolBackgroundColor'))
    set(hObject,'BackgroundColor','white');
end



function Capacitance_Callback(hObject, eventdata, handles)
% hObject    handle to text10 (see GCBO)
% eventdata  reserved - to be defined in a future version of MATLAB
% handles    structure with handles and user data (see GUIDATA)

% Hints: get(hObject,'String') returns contents of text10 as text
%        str2double(get(hObject,'String')) returns contents of text10 as a
double


% --- Executes during object creation, after setting all properties.
function Capacitance_CreateFcn(hObject, eventdata, handles)
% hObject    handle to text10 (see GCBO)
% eventdata  reserved - to be defined in a future version of MATLAB
% handles    empty - handles not created until after all CreateFcns called

% Hint: edit controls usually have a white background on Windows.
%       See ISPC and COMPUTER.
if ispc && isequal(get(hObject,'BackgroundColor'),
get(0,'defaultUicontrolBackgroundColor'))
    set(hObject,'BackgroundColor','white');
end



function Ideality_factor_Callback(hObject, eventdata, handles)
% hObject    handle to Ideality_factor (see GCBO)
% eventdata  reserved - to be defined in a future version of MATLAB
% handles    structure with handles and user data (see GUIDATA)

% Hints: get(hObject,'String') returns contents of Ideality_factor as text
%        str2double(get(hObject,'String')) returns contents of
Ideality_factor as a double


% --- Executes during object creation, after setting all properties.
function Ideality_factor_CreateFcn(hObject, eventdata, handles)
```

```
% hObject    handle to Ideality_factor (see GCBO)
% eventdata  reserved - to be defined in a future version of MATLAB
% handles    empty - handles not created until after all CreateFcns called

% Hint: edit controls usually have a white background on Windows.
%       See ISPC and COMPUTER.
if ispc && isequal(get(hObject,'BackgroundColor'),
get(0,'defaultUicontrolBackgroundColor'))
    set(hObject,'BackgroundColor','white');
end



function Current_time_Callback(hObject, eventdata, handles)
% hObject    handle to Current_time (see GCBO)
% eventdata  reserved - to be defined in a future version of MATLAB
% handles    structure with handles and user data (see GUIDATA)

% Hints: get(hObject,'String') returns contents of Current_time as text
%        str2double(get(hObject,'String')) returns contents of Current_time
as a double


% --- Executes during object creation, after setting all properties.
function Current_time_CreateFcn(hObject, eventdata, handles)
% hObject    handle to Current_time (see GCBO)
% eventdata  reserved - to be defined in a future version of MATLAB
% handles    empty - handles not created until after all CreateFcns called

% Hint: edit controls usually have a white background on Windows.
%       See ISPC and COMPUTER.
if ispc && isequal(get(hObject,'BackgroundColor'),
get(0,'defaultUicontrolBackgroundColor'))
    set(hObject,'BackgroundColor','white');
end



function Msg_Callback(hObject, eventdata, handles)
% hObject    handle to Msg (see GCBO)
% eventdata  reserved - to be defined in a future version of MATLAB
% handles    structure with handles and user data (see GUIDATA)

% Hints: get(hObject,'String') returns contents of Msg as text
%        str2double(get(hObject,'String')) returns contents of Msg as a
double


% --- Executes during object creation, after setting all properties.
function Msg_CreateFcn(hObject, eventdata, handles)
% hObject    handle to Msg (see GCBO)
% eventdata  reserved - to be defined in a future version of MATLAB
% handles    empty - handles not created until after all CreateFcns called
```

```
% Hint: edit controls usually have a white background on Windows.
%       See ISPC and COMPUTER.
if ispc && isequal(get(hObject,'BackgroundColor'),
get(0,'defaultUicontrolBackgroundColor'))
    set(hObject,'BackgroundColor','white');
end


% --- Executes on selection change in COM.
function COM_Callback(hObject, eventdata, handles)
% hObject    handle to COM (see GCBO)
% eventdata  reserved - to be defined in a future version of MATLAB
% handles    structure with handles and user data (see GUIDATA)

% Hints: contents = cellstr(get(hObject,'String')) returns COM contents as
cell array
%        contents{get(hObject,'Value')} returns selected item from COM
COM = get(findobj(hObject,'Tag','COM'),'Value');
switch COM
    case 1
        handles.COM = 'COM1';
    case 2
        handles.COM = 'COM2';
    case 3
        handles.COM = 'COM3';
    case 4
        handles.COM = 'COM4';
    case 5
        handles.COM = 'COM5';
end
handles.output = hObject;
guidata(hObject, handles);
% --- Executes during object creation, after setting all properties.
function COM_CreateFcn(hObject, eventdata, handles)
% hObject    handle to COM (see GCBO)
% eventdata  reserved - to be defined in a future version of MATLAB
% handles    empty - handles not created until after all CreateFcns called

% Hint: popupmenu controls usually have a white background on Windows.
%       See ISPC and COMPUTER.
if ispc && isequal(get(hObject,'BackgroundColor'),
get(0,'defaultUicontrolBackgroundColor'))
    set(hObject,'BackgroundColor','white');
end



function Channels_Callback(hObject, eventdata, handles)
% hObject    handle to Channels (see GCBO)
% eventdata  reserved - to be defined in a future version of MATLAB
% handles    structure with handles and user data (see GUIDATA)

% Hints: get(hObject,'String') returns contents of Channels as text
%        str2double(get(hObject,'String')) returns contents of Channels as a
double
```

```
handles.Channels_num =
str2double(get(findobj(hObject,'Tag','Channels'),'String'));
handles.output = hObject;
guidata(hObject, handles);

% --- Executes during object creation, after setting all properties.
function Channels_CreateFcn(hObject, eventdata, handles)
% hObject    handle to Channels (see GCBO)
% eventdata  reserved - to be defined in a future version of MATLAB
% handles    empty - handles not created until after all CreateFcns called

% Hint: edit controls usually have a white background on Windows.
%       See ISPC and COMPUTER.
if ispc && isequal(get(hObject,'BackgroundColor'),
get(0,'defaultUicontrolBackgroundColor'))
    set(hObject,'BackgroundColor','white');
end



% --- Executes during object deletion, before destroying properties.
function text12_DeleteFcn(hObject, eventdata, handles)
% hObject    handle to text12 (see GCBO)
% eventdata  reserved - to be defined in a future version of MATLAB
% handles    structure with handles and user data (see GUIDATA)


% --- Executes on selection change in popupmenu2.
function popupmenu2_Callback(hObject, eventdata, handles)
% hObject    handle to popupmenu2 (see GCBO)
% eventdata  reserved - to be defined in a future version of MATLAB
% handles    structure with handles and user data (see GUIDATA)

% Hints: contents = cellstr(get(hObject,'String')) returns popupmenu2
contents as cell array
%        contents{get(hObject,'Value')} returns selected item from popupmenu2


% --- Executes during object creation, after setting all properties.
function popupmenu2_CreateFcn(hObject, eventdata, handles)
% hObject    handle to popupmenu2 (see GCBO)
% eventdata  reserved - to be defined in a future version of MATLAB
% handles    empty - handles not created until after all CreateFcns called

% Hint: popupmenu controls usually have a white background on Windows.
%       See ISPC and COMPUTER.
if ispc && isequal(get(hObject,'BackgroundColor'),
get(0,'defaultUicontrolBackgroundColor'))
    set(hObject,'BackgroundColor','white');
end
```

References

[1] Thevenot, Daniel; Toth, Klara; Wilson, George, Electrochemical biosensors: recommended definitions and classification., Pure and Applied Chemistry, International Union of Pure and Applied Chemistry, 1999, pp. pp.2333-2348.

[2] Birch, Brian, Introduction to Biosensors.

[3] Campbell T, Charles, "Surface Plasmon Resonance (SPR) Biosensor Development," University of Washington, [Online]. Available: https://depts.washington.edu/campbelc/projects/plasmon.pdf. [Accessed 25 March 2015].

[4] Jang, Byungchul; Cao, Peiyan; Chevalier, Aaron; Ellington, Andrew; Hassibi, Arjang, "A CMOS Fluorescent-Based Biosensor Microarray," in *ISSCC Medical*, Texas, 2009.

[5] Long,Feng;Zhu,Anna; Shi,Hanchang, "Recent Advances in Optical Biosensors for Environmental Monitoring and Early Warning," *Sensors,* vol. 14248220, p. p13928, 2013.

[6] Hauck ,Sabine; Drost, Stephan; Prohaska,Elke;Wolf,Hans;Dubel,Stefan, "Analysis of Protein Interactions Using a Quartz Crystal Microbalance Biosensor".

[7] K.-U. Kirstein, M. Z. Y. Li, C. Vancura, T. Volden, W. H. Song, J. Lichtenberg and A. Hierlemannn, "Cantilever-Based Biosensors in CMOS Technology," vol. 02, pp. 210-214, 2005.

[8] Wang, Hua; Chen, Yan; Hassibi, Arjang; Scherer, Axel; Hajimiri, Ali, "A Frequency-Shift CMOS Magnetic Biosensor Array with Single-Bead Sensitivity and No External Magnet," in *ISSCC 2009*, Pasadena, CA, 2009.

[9] Biosensor Academy, "biosensoracademy.com," [Online]. Available: http://www.biosensoracademy.com/eng/readarticle.php?article_id=11. [Accessed 16 February 2015].

[10] Daniel, Jonathan S., An Integrated Impedance Biosensor Array, 2010.

[11] Voldman, Joel; Brandt, Brian; Wu, Dan, "Several Presentations on Biosensors," Boston, 2014.

[12] Guan,Jian-Guo;Miao,Yu-Qing;Zhang Qing-Jie, "Impedimetric Biosensors," *Journal of BioScience and BioEngineering,* vol. 97, no. 4, pp. 219-226, 2004.

[13] Agilent Technologies, "Agilent Impedance Measurement Handbook," [Online]. Available: cp.literature.agilent.com/litweb/pdf/5950-3000.pdf. [Accessed 19 February 2015].

[14] Rossi,Michele;Bennati,Marco; Thei,Federico;Tartagni,Marco, "A Low-cost and Portable System for Real-time Impedimetric Measurements and Impedance Spectroscopy of Sensor," in *The Third International Conference on Sensor Device Technologies and Applications*, 2012.

[15] K. Witt and J. D. Cristina, "Apparatus for low power measurement of complex impedance vs frequency for biomedical instrumentation.". United States of America 2014.

[16] "www.radioing.com/eengineer/pcb-tips.html," [Online]. Available: www.radioing.com/eengineer/pcb-tips.html. [Accessed 7 April 2015].

[17] Bottazzi, Barbara; Fornasari, Lucia; Frangolho, Ana; Guidicatti, Silvia; Mantovani, Alberto, "Multiplexed label-free optical biosensor for medical diagnostics," *Journal of Biomedical Optics,* vol. 017006, p. 19(1), 2013.